



INTERNATIONAL ATOMIC ENERGY AGENCY

INDC(CCP)-424

Distr.: L0

---

**I N D C      INTERNATIONAL NUCLEAR DATA COMMITTEE**

---

**SELECTED ARTICLES TRANSLATED FROM  
JADERNYE KONSTANTY (NUCLEAR CONSTANTS)**

(Series: Nuclear Constants Issue No. 1 1999)

Translated by the IAEA

March 2000

Printed by the IAEA in Austria  
March 2000

**INDC(CCP)-424**  
**Distr.: L0**

**SELECTED ARTICLES TRANSLATED FROM  
JADERNYE KONSTANTY (NUCLEAR CONSTANTS)**

(Series: Nuclear Constants Issue No. 1 1999)

March 2000

## CONTENTS

<b>Re-Evaluated Resonance Parameters of <math>^{233}\text{U}</math>.....</b>	5
<i>G.B. Morogovskij</i>	
<b>Resolved Resonance Parameters for <math>^{238}\text{Np}.....</math></b>	19
<i>G.B. Morogovskij</i>	
<b>Level Density Parameters for the Back-Shifted Fermi Gas Model in the Mass Range <math>24 \leq A \leq 250.....</math></b>	27
<i>V.I. Plyaskin, R.A. Kosilov</i>	
<b>Phase Analysis of the <math>p^3\text{He}</math> and <math>pT</math> Elastic Scattering Cross-Sections in the 0-20 MeV Energy Region.....</b>	45
<i>L.M. Lazarev, B.M. Dzyuba</i>	

99-11877 (90)

Translated from Russian

UDC 539.163

SERIYA: JADERNYE KONSTANTY, Vypusk 1, 1999, s. 9  
(Series: Nuclear Constants, Issue No. 1 1999, p. 9)

## **RE-EVALUATED RESONANCE PARAMETERS of $^{233}\text{U}$**

G.B. Morogovskij

Institute for Radiation Physics and Chemistry Problems  
National Academy of Sciences, Republic of Belarus

### **ABSTRACT**

The multilevel Breit-Wigner parameters and smooth file were obtained for the representation of neutron cross-sections in the  $10^{-5}$ -201 eV energy region pursuant to the re-evaluation of the  $^{233}\text{U}$  evaluated nuclear data file (BROND) in the resolved resonance region. The resonance parameters in the 150-201 eV energy region were obtained for the first time.

In this paper, previously obtained  $^{233}\text{U}$  parameters [1] in the resolved resonance region are re-evaluated. This re-evaluation is necessary because the potential of computer technology has increased considerably since the creation of the  $^{233}\text{U}$  evaluated nuclear data file (BROND) [2], with the result that evaluated resonance parameters can be obtained now at a higher level and the boundaries of the resolved resonance region extended. This paper attempts to put forward an agreed set of multilevel Breit-Wigner resonance parameters that adequately describe the existing experimental measurements of the total cross-section and the fission and radiative capture cross-sections in the  $10^{-5}$ -201 eV energy region. To perform the calculations, previously used computer programs [1, 3] have been modified to take account of the new capabilities of computer technology, and some new programs have been developed enabling the quality of the parameters obtained to be improved significantly.

In recent years, no new measurements have been made in the region under consideration; thus, the same experimental data and cross-section values at the thermal point have been used in our work as in the previous evaluation [1, 3]. In Ref. [3], the pointwise behaviour of the  $\sigma_t(E)$ ,  $\sigma_f(E)$  and  $\sigma_\gamma(E)$  cross-sections was obtained in the  $10^{-5}$ -1 eV energy region file 3, and the energy values 1 and 100 eV were adopted as the boundaries of the resolved resonance region. In this paper, the evaluated cross-section values and  $\sigma_\gamma^{2200}$  values from study [2] have been used to obtain the parameters of resonances with energies of less than 1 eV. Only one negative resonance was needed, in conjunction with the full set of evaluated resonance parameters, to achieve a high level of agreement between the calculated cross-section values up to 1 eV and both the measurements in this region used in Ref. [3] and the evaluated cross-sections [2]. The only exception to this is the value  $\sigma_\gamma^{2200} = 46.9$  b, which

is 3.3% higher than the value  $\sigma_{\gamma}^{2200} = 45.4$  b used when obtaining the parameters. In the ENDF/B-VI [4] and JEF-2 [5] evaluations, and in Ref. [2], a pointwise representation of cross-sections was used up to 1 eV, yielding the value  $\sigma_{\gamma}^{2200} = 45.8-45.9$  b; in the JENDL-3.2 evaluation [6], a clearly non-physical and anomalously low value of  $\Gamma_{\gamma} = 0.9$  meV for  $E_{\gamma} = 0.44$  eV was taken to obtain  $\sigma_{\gamma}^{2200} = 45.25$  b, the average value of  $\Gamma_{\gamma}$  for this evaluation being 41.5 meV, and the minimum value  $\Gamma_{\gamma} = 17.3$  meV. In view of the low level of accuracy of the measurements of  $\sigma_{\gamma}(E)$  performed by Weston et al. [7] in the region under consideration, the value  $\sigma_{\gamma}^{2200} = 49.6$  b yielded by parametrization may be considered acceptable.

The following series of experimental data were used to obtain the resonance parameters in the 1-200.2 eV energy interval:

- for  $\sigma_t$  Kolar et al. [8];
- for  $\sigma_f$  Deruytter et al. [9], Nizamuddin et al. [10];
- for  $\sigma_{\gamma}$  Weston et al. [11].

Since the energy scales of different experiments do not always coincide, for the parametrization over the whole energy region under consideration, Ref. [9] was taken as a basis in the  $10^{-5}$ -6.7 eV interval and Ref. [10] in the 6.7-201 eV interval. The shift in the energy scales in the remaining sources was calculated for all well defined resonances over the whole energy region.

The data used for the parametrization were normalized in the following manner:

- The evaluated data and thermal cross-sections from Ref. [2] used to calculate the parameters up to 1 eV agreed with the cross-section values in  $E = 0.0253$  eV adopted in this paper and no renormalization was required;
- Deruytter's fission cross-section measurements [9] were renormalized to  $\sigma_f^{2200} = 529.6$  b, the value used in Ref. [2] and in this paper;
- Weston's fission cross-sections [11], although not used in the parametrization, were renormalized to the new Deruytter fission cross-section values in accordance with the integral values in the intervals used in Ref. [9] in the 0.75-30.3 eV region;
- Nizamuddin's fission cross-sections [10] were renormalized to the new Weston fission cross-section values in the corresponding Ref. [9] intervals in the 9-1000 eV region;

- Weston's radiative capture cross-sections [11] were renormalized using the same renormalization coefficient as for Weston's fission cross-sections [11] in order to retain the  $\alpha(E)$  value.

The parameters were calculated using multilevel Breit-Wigner formalism and all the above-mentioned data, taking into account the authors' sample temperature values and the energy resolutions of the experiments. The highest statistical weighting was given to Nizamuddin's fission cross-sections [10]; Kolar's [8] and Deruytter's [9] measurements were given a slightly lower weighting, and Weston's data [11] were given the lowest statistical weighting.

Table I shows the resonance parameters we obtained. Comparing the data in Table I with the BNL-325 [12] and JENDL-3.2 [6] evaluations, we can see that, up to 125 eV, the number of observed resonances in BNL-325 and this paper is practically identical (177 and 182 respectively), whereas 155 resonances are used in this region in JENDL-3.2. In the 125-150 eV region, 24 resonances are given in the JENDL-3.2 evaluation, whereas there are 34 in this paper; in the 150-201 eV interval the parameters of 65 resonances were obtained for the first time.

The following average resonance parameter and thermal cross-section values may be obtained using the values given in Table I (calculation performed using the PSYCHE and INTER programs [13]):

$$\langle \Gamma_n^0 \rangle = 0.1316 \text{ meV} \quad \langle D \rangle = 0.7127 \text{ eV}$$

$$\langle \Gamma_\gamma \rangle = 40 \text{ meV} \quad S^0 = 0.9196 \times 10^{-4}$$

$$\langle \Gamma_f \rangle = 417.9 \text{ meV}$$

$$\sigma_t^{2200} = 587.6 \text{ b}$$

$$\sigma_\gamma^{2200} = 46.90 \text{ b} \quad g_\gamma = 1.00212 \quad I_\gamma(0.5-200 \text{ eV}) = 133.604 \text{ b}$$

$$\sigma_f^{2200} = 529.6 \text{ b} \quad g_f = 1.00272 \quad I_f(0.5-200 \text{ eV}) = 708.278 \text{ b}$$

$$\sigma_n^{2200} = 11.1 \text{ b}$$

Taking into account possible missing levels yields the following values for  $\langle D \rangle_{ev}$  and  $\langle \Gamma_n^0 \rangle_{ev}$ :

$$\langle D \rangle_{ev} = 0.515 \pm 0.013 \text{ eV} \quad \langle \Gamma_n^0 \rangle_{ev} = 0.111 \pm 0.008 \text{ meV},$$

where  $S^0_{ev} = (1.079 \pm 0.080) \times 10^{-4}$ .

From Table I, it can be seen that there is an excess of fission widths with high values of  $\Gamma_f$  ( $\Gamma_f$  greater than  $2.8 * \langle \Gamma_f \rangle$ ) distributed over the energy intervals in the following manner:

0-50 eV-	8	100-150 eV-	5
50-100 eV-	2	150-200 eV-	10

The majority of the resonances with these unusually large  $\Gamma_f$  values are unresolved doublets in the experiment, although it is not possible to determine which of these resonances are doublets on the basis of the information available.

Since it is not possible to determine the spin of each specific resonance from the existing experimental cross-section measurements, the spin values were calculated on the basis of the following criteria:

- 1) The number of resonances for a given spin is proportional to  $2J + 1$ ;
- 2) The number of neighbouring resonances with the same value of  $J$  is no more than 3;
- 3)  $\langle\Gamma_f\rangle_{J=2}$  is greater than  $\langle\Gamma_f\rangle_{J=3}$ ;
- 4) Both systems of resonances should agree with Wigner's distribution.

The resonance parameters we obtained are better than the previous evaluations [2, 4-6, 12]; they describe the energy dependence of all the experimental and evaluated cross-sections used over the whole energy interval under consideration, taking into account the authors' sample temperature values and the energy resolutions. Fig. 1 shows the experimental measurements of  $\sigma_t(E)$  [8],  $\sigma_f(E)$  [10] and  $\sigma_\gamma(E)$  [11], together with the corresponding calculated cross-section values obtained from the parameters in Table I in the 125-201 eV energy interval. Calculation of the smooth file shows that it is sufficient to use 59 points over the entire interval under consideration to improve the level of agreement between the experimental and calculated cross-section values; the most notable contribution to the cross-section is in the 2.37-3.4 eV, 3.6-18 eV and 107.5-108.2 eV energy intervals. Table II shows the smooth file, which is recommended for use together with the parameters in Table I to obtain reliable calculated cross-section values in the  $10^{-5}$ -201 eV energy interval.

TABLE I. RESONANCE PARAMETERS OF  $^{233}\text{U}$ 

$E_r$ , eV	J	$\Gamma_n$ , meV	$\Gamma_\gamma$ , meV	$\Gamma_f$ , meV
-0.844586	3	0.31689	24.27	213.140
0.205	3	0.00011	40.08	23.624
0.450	3	0.01142	25.54	897.010
1.550	2	0.14959	48.06	462.000
1.790	3	0.20073	43.06	138.920
2.170	2	0.35767	29.03	1270.800
2.295	2	0.19212	47.11	42.770
3.450	2	0.03475	28.33	140.290
3.620	3	0.07113	32.62	90.880
4.760	3	0.25502	39.04	824.400
5.890	3	0.06412	40.98	204.430
6.270	2	0.40418	43.05	1009.500
6.640	3	0.10407	48.05	171.040
6.823	3	0.68691	36.64	96.886
7.500	3	0.02082	38.14	78.962
7.910	2	0.06480	40.07	1259.900
8.640	3	0.05794	38.20	414.160
9.260	3	0.08384	39.17	196.140
9.710	3	0.12611	52.00	841.250
10.380	2	1.92509	43.49	263.810
10.860	2	0.05303	44.36	247.970
11.310	2	0.21989	36.74	314.220
11.890	3	0.30585	51.49	1245.000
12.800	2	1.78721	39.01	277.280
13.450	3	0.03477	38.35	46.375
13.730	3	0.28740	38.32	227.060
13.950	3	0.01096	33.44	139.830
15.330	2	0.48442	33.83	50.366
15.470	3	0.33518	42.27	130.530
15.820	3	0.48115	34.44	1235.000
16.200	2	0.77023	46.42	317.420
16.550	2	0.82390	39.05	171.760
17.280	3	0.00063	36.58	0.020
17.630	3	0.00126	56.02	80.896
17.970	3	0.17115	36.47	101.540
18.280	2	0.57091	51.98	1248.800
18.480	2	0.08766	46.45	35.314
18.940	3	1.49271	36.98	241.290
19.630	3	0.27843	43.25	1256.500
20.580	3	0.75593	47.76	301.620
21.580	2	0.50177	26.42	516.270
21.870	3	0.94202	42.16	146.150
22.330	3	2.90160	36.89	316.730
22.910	3	0.89460	29.26	873.150
23.770	2	0.59407	35.58	375.460
24.260	3	0.28869	35.81	722.620
25.260	2	0.82716	42.85	229.520
25.780	2	1.20125	35.54	1124.800

26.250	3	0.05738	44.17	235.860
26.610	3	0.32585	43.72	192.030
26.980	2	0.12144	35.44	362.400
27.430	3	0.03033	40.03	84.428
27.700	2	0.00292	39.14	281.730
28.070	3	0.52493	29.78	849.920
28.280	2	0.12729	36.64	45.460
29.060	3	1.66702	37.40	526.310
29.580	3	0.12233	36.95	188.360
30.350	3	0.04253	44.74	99.621
30.720	2	0.79574	40.28	227.140
31.330	2	0.49466	30.48	386.690
31.690	3	0.32664	53.16	512.200
32.010	2	1.17924	35.89	183.040
33.140	2	1.48891	41.84	1010.000
33.550	3	0.00756	39.72	14.554
33.950	3	0.97925	30.48	1026.000
34.510	2	1.99814	36.72	716.480
35.200	3	0.10589	35.54	78.534
35.400	3	0.04533	39.43	71.631
35.750	2	0.83170	45.03	740.720
36.530	2	1.31705	36.67	165.280
37.200	3	0.07193	31.73	33.214
37.480	2	0.75696	31.80	292.320
39.330	3	0.51854	35.84	739.400
39.830	3	0.64416	45.61	920.350
40.410	2	0.74172	32.52	664.090
41.030	3	0.34217	48.38	148.330
41.750	3	0.00216	28.45	134.770
42.090	2	0.43339	28.48	1271.400
42.620	3	0.59187	37.25	123.120
43.500	3	0.29897	44.27	222.720
44.520	3	0.26062	41.87	457.290
45.250	3	0.00049	32.63	133.270
46.090	3	0.34018	42.87	77.860
46.500	2	0.31728	32.97	1265.900
47.200	2	1.00908	45.23	384.910
48.680	3	1.76589	48.09	91.225
49.100	2	0.72406	33.01	568.360
50.400	3	0.56991	36.40	750.680
51.000	2	0.11031	33.04	491.900
52.000	3	0.03759	33.36	175.290
53.030	3	0.51259	33.38	211.830
53.320	2	0.25330	48.46	280.540
53.940	2	0.14976	51.08	223.580
54.010	2	2.28139	48.71	573.840
54.410	3	0.01907	35.65	206.380
54.750	2	1.41086	43.01	153.940
55.200	3	0.28786	28.58	612.880
55.950	3	1.59567	46.21	502.000
56.440	3	1.54517	45.92	386.620

56.880	2	0.01924	33.49	122.880
57.480	3	3.32606	39.39	928.040
58.180	2	0.61730	33.59	980.550
58.510	3	0.77913	38.47	240.410
59.100	2	0.06185	49.60	212.600
60.100	3	0.04536	56.21	28.934
60.420	2	0.21976	53.65	504.820
60.950	2	0.43085	41.70	300.080
61.380	3	1.62153	37.49	407.810
62.590	3	1.37955	43.25	71.864
63.490	2	0.12739	33.69	339.920
64.030	2	1.20190	41.94	372.870
64.440	3	1.15322	44.29	159.160
65.090	2	0.74393	36.11	246.400
65.490	2	0.51787	36.07	662.030
66.700	3	0.77779	54.53	932.520
67.300	3	0.07842	33.64	439.270
67.980	3	0.39166	38.15	277.250
69.230	2	2.77872	44.38	849.900
70.190	2	2.41584	36.20	499.150
71.750	2	0.32525	28.87	403.080
72.150	3	0.49106	49.34	830.670
73.440	3	1.62684	45.07	66.772
74.020	2	6.40752	43.24	502.230
75.000	3	0.52893	41.10	100.800
75.490	2	4.08240	42.95	252.860
76.770	3	0.45339	34.00	658.750
78.180	3	2.23611	41.87	598.820
78.460	3	0.11426	34.00	264.900
79.000	2	0.55668	38.75	503.580
79.780	2	3.23184	38.95	482.220
81.600	3	1.17127	34.09	1157.100
82.400	3	1.58597	47.02	510.570
82.780	3	2.68817	46.45	50.810
84.650	2	0.21473	28.95	369.170
85.220	3	0.88445	34.83	450.270
85.800	2	0.35935	35.17	1263.700
86.780	2	0.01048	43.43	47.947
87.130	3	0.31366	41.59	171.570
87.700	3	0.00008	49.52	154.200
88.880	3	2.10240	45.70	372.280
89.850	2	0.80945	47.76	452.180
90.540	3	7.13297	47.57	124.880
91.100	3	0.22191	40.56	102.180
91.700	2	1.38758	35.19	1263.500
92.670	2	1.16256	42.86	292.480
93.250	2	0.85085	35.35	655.100
93.770	3	1.34787	36.34	47.933
95.220	3	1.37191	43.12	109.260
96.300	3	2.26423	54.42	1149.000
97.150	2	0.70490	39.65	419.710

97.820	3	5.43120	52.49	63.698
98.580	2	3.26328	41.09	417.130
99.400	3	1.14132	36.84	589.940
99.950	2	3.31296	43.23	502.020
101.290	3	0.00281	47.88	309.500
102.890	3	1.17087	33.21	213.040
104.790	2	1.55146	40.91	200.680
105.230	3	0.11325	47.28	18.910
105.950	3	1.23650	30.82	37.889
106.510	2	8.91840	55.72	835.710
106.950	3	1.11139	35.73	100.040
107.830	2	0.50378	37.96	306.280
108.050	3	2.13034	39.45	993.710
108.800	2	0.17837	33.15	200.410
109.360	2	4.04400	36.73	264.910
109.980	3	0.57386	32.72	230.460
110.880	3	5.06674	39.02	370.370
112.530	2	2.34108	51.07	573.190
113.100	3	0.24360	39.49	99.893
113.550	3	1.85606	51.14	650.300
114.240	3	3.68880	40.04	939.690
114.560	2	2.31017	42.69	234.670
115.800	3	0.20354	33.13	33.399
117.000	2	0.67025	33.06	622.970
117.920	2	8.53152	36.12	249.840
119.450	2	2.15513	42.23	143.310
120.020	3	1.65631	45.17	1254.000
121.190	2	2.02118	45.53	468.130
122.050	3	0.73397	31.45	43.335
122.670	3	1.46191	43.33	670.310
123.200	2	0.22344	39.42	138.410
123.600	3	0.18043	34.49	60.313
124.120	3	5.05200	37.95	237.820
125.200	2	2.02306	40.05	1256.500
126.060	3	0.88617	45.66	291.460
127.350	2	0.27084	34.51	414.000
127.630	3	0.03601	32.61	16.469
128.050	3	1.25902	40.69	787.000
128.400	3	0.00395	38.38	0.049
128.800	2	0.96062	42.55	1160.400
129.500	2	0.16355	60.69	414.000
130.350	2	0.31555	36.51	143.170
131.050	3	0.01191	45.80	640.030
131.650	3	0.01041	38.27	18.911
132.410	3	1.54920	38.33	1006.300
133.200	2	4.51008	38.12	253.200
133.850	3	3.05297	29.51	828.100
135.350	2	5.42568	31.81	295.720
136.400	2	1.02955	39.04	566.620
138.290	3	0.02520	43.65	414.000
139.590	3	1.06733	33.17	1265.600

140.150	2	0.16116	38.12	525.660
140.450	2	0.22130	36.52	32.259
140.850	3	1.06701	39.39	552.960
141.850	3	2.82463	38.98	505.190
142.840	2	3.75096	37.90	73.817
143.600	2	0.02411	44.98	51.980
144.200	2	1.35996	46.07	687.450
144.750	3	0.08994	42.81	39.264
145.430	3	4.30680	46.88	81.614
146.100	2	0.08246	36.63	43.135
146.880	3	0.20775	42.76	414.000
147.350	2	1.05823	45.61	1253.500
147.800	3	0.02342	33.94	3.705
148.400	3	0.05891	35.55	0.106
148.700	3	1.55837	46.93	1251.200
149.180	2	4.35528	44.65	496.990
149.700	3	0.37550	41.83	204.520
150.500	3	0.09806	35.73	167.410
150.800	3	0.05538	42.25	1257.700
151.200	2	1.29038	38.46	1259.800
151.600	3	4.69509	49.31	995.730
152.200	3	0.34049	34.86	246.410
152.700	3	0.26314	41.61	12.836
153.100	2	0.06647	43.57	266.960
153.600	3	0.45559	55.16	62.185
154.000	3	0.42708	39.98	316.030
154.900	3	0.03217	40.45	32.230
155.600	2	1.77984	36.37	139.430
156.600	3	0.21453	36.42	414.000
156.850	2	3.32976	31.86	503.720
158.330	2	0.10767	32.53	21.030
159.100	2	0.16351	41.93	57.142
159.400	3	0.00843	38.95	0.311
160.700	3	0.04909	36.24	116.320
161.200	3	0.59405	44.35	1254.700
161.800	2	4.15584	45.18	376.790
162.480	3	1.42589	50.57	174.530
163.200	2	3.46056	38.70	1258.100
164.800	3	1.50327	39.70	49.976
165.180	3	5.14491	36.77	247.440
165.800	3	0.86446	38.16	82.707
167.400	2	5.12160	40.08	695.280
167.700	3	1.15486	44.21	40.864
168.580	2	3.42816	56.53	115.690
169.200	3	1.27368	35.69	188.440
169.600	2	0.70752	43.56	275.830
170.800	3	0.00966	32.53	1.044
171.100	3	2.83577	44.29	684.480
171.700	2	0.12639	41.93	33.312
172.900	3	0.00396	36.93	225.550
173.600	3	1.48512	41.56	1256.200

174.300	3	0.11389	38.16	8.372
175.000	2	7.91448	40.89	975.550
175.700	3	0.32642	40.22	2.879
176.880	3	0.06674	31.28	20.841
178.100	2	2.98824	33.64	1242.100
179.100	3	0.08401	41.86	87.380
180.850	2	0.26220	30.79	31.390
181.400	3	0.52882	36.48	82.456
182.450	2	0.32417	38.38	414.000
182.750	3	0.92179	42.26	97.031
184.050	3	0.65364	44.15	1116.100
184.550	2	0.88327	33.92	84.894
185.080	3	0.62618	40.69	384.570
185.650	2	0.65808	32.18	286.160
186.350	3	0.15061	37.23	390.060
187.570	3	3.38400	38.31	639.650
189.450	3	10.22330	38.81	1249.300
190.050	2	0.33118	48.78	414.000
190.850	3	3.33617	33.96	465.110
191.800	2	3.17448	44.53	1269.000
192.400	3	0.62765	41.58	254.160
193.100	3	1.51365	50.63	762.450
193.500	3	0.02685	32.53	41.607
194.450	2	1.49122	33.95	1264.800
195.300	3	0.12072	41.93	171.420
196.150	2	5.99472	52.34	1242.700
196.520	3	0.73059	41.06	47.203
197.450	2	5.92560	50.30	154.380
198.000	3	0.49389	39.08	73.268
198.800	3	2.35954	31.57	530.910
200.140	2	3.93456	46.07	460.810

TABLE II. SMOOTH FILE FOR RESONANCE PARAMETERS OF  $^{233}\text{U}$ 

E, eV	$\sigma_t$ , barns	$\sigma_f$ , barns	$\sigma_{\gamma}$ , barns
0.00005	0.0000	0.0000	0.0000
2.3704	0.0000	0.0000	0.0000
2.3911	-93.1970	-86.8260	-6.3712
2.5097	-105.2100	-99.5410	-5.6669
2.6998	-57.8010	-55.3030	-2.4980
2.8079	-40.5580	-37.9480	-2.6101
3.2356	9.5950	12.3080	-2.7128
3.4040	0.0000	0.0000	0.0000
13.5900	0.0000	0.0000	0.0000
13.7300	-4.3614	-4.3367	-0.0247
13.9210	3.2488	7.4893	-4.2405
14.1490	-0.7999	-0.8482	0.0484
14.9000	-16.0320	-19.7490	3.7175
15.1100	0.0000	0.0000	0.0000
16.5900	0.0000	0.0000	0.0000
16.7100	19.5140	19.2590	0.2557
17.0840	-6.6858	-7.0428	0.3571
17.8000	-10.2880	-13.3290	3.0411
18.0100	0.0000	0.0000	0.0000
32.3020	0.0000	0.0000	0.0000
32.5750	-11.3680	-9.8704	-1.4978
32.8060	0.0000	0.0000	0.0000
37.8040	0.0000	0.0000	0.0000
38.4050	-3.7707	-3.9604	0.1898
38.6570	-4.0045	-4.8791	0.8745
38.8270	0.0000	0.0000	0.0000
38.9280	2.8558	2.9446	-0.0888
39.0910	0.0000	0.0000	0.0000
44.7000	0.0000	0.0000	0.0000
45.2060	1.5316	1.5117	0.0199
45.7760	-4.6596	-3.4769	-1.1828
45.9080	0.0000	0.0000	0.0000
47.6030	0.0000	0.0000	0.0000
47.7130	-1.3000	0.1558	-1.4559
47.8320	0.0000	0.0000	0.0000
48.0730	-5.0080	-5.2045	0.1965
48.3000	0.0000	0.0000	0.0000
94.1720	0.0000	0.0000	0.0000

94.5420	-2.8347	-1.8963	-0.9385
94.6220	-3.0197	-3.4414	0.4218
94.7910	0.0000	0.0000	0.0000
103.4000	0.0000	0.0000	0.0000
103.5300	-4.9900	-5.0128	0.0228
103.9100	-3.7790	-3.8793	0.1003
104.1000	0.0000	0.0000	0.0000
107.4600	0.0000	0.0000	0.0000
107.5100	-13.5220	-13.5220	0.0000
108.0100	4.8643	4.3351	0.5293
108.2100	0.0000	0.0000	0.0000
109.6000	0.0000	0.0000	0.0000
109.7400	9.9604	9.3455	0.6149
109.8900	6.3928	0.2983	6.0945
110.0900	4.6243	0.2845	4.3398
110.2000	0.0000	0.0000	0.0000
114.6800	0.0000	0.0000	0.0000
115.2300	-7.8152	-8.9142	1.0990
115.2500	-7.7822	-6.7356	-1.0466
115.7800	0.0000	0.0000	0.0000
201.0000	0.0000	0.0000	0.0000

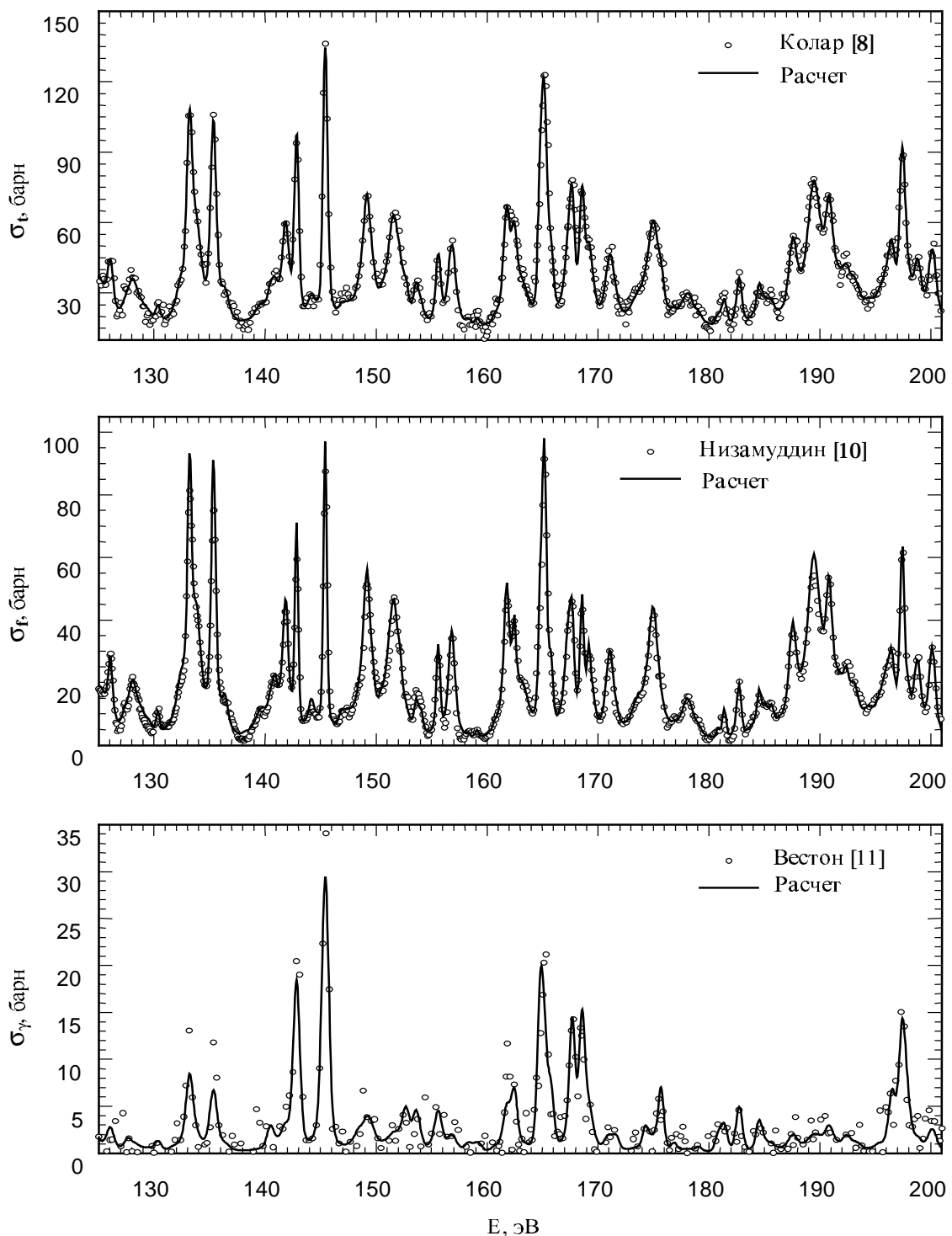


FIG. 1. Comparison of the experimental  $^{233}\text{U}$  cross-sections and those calculated using the parameters in Table I in the 125-201 eV energy interval. Legend: a) y-axis -  $\sigma_t$ ; barns; x-axis - E; eV; ° - Kolar [8]; — calculation; b) y-axis -  $\sigma_f$ ; barns; x-axis - E; eV; ° - Nizamuddin [10]; — calculation; c) y-axis -  $\sigma_\gamma$ ; barns; x-axis - E; eV; ° - Weston [11]; — calculation.

## REFERENCES

- [1] MOROGOVSKIJ, G.B., Voprosy Atomnoj Nauki i Tekhniki, Seriya: Jadernye Konstanty 1 (1991) 30.
- [2] BAKHANOVICH, L.A., KLEPATSKIJ, A.B., MASLOV, V.M., et al., Report INDC(BLR)-001, IAEA, Vienna (1993).
- [3] BAKHANOVICH, L.A., MOROGOVSKIJ, G.B., Voprosy Atomnoj Nauki i Tekhniki, Seriya: Jadernye Konstanty 1 (1991) 26.
- [4] DUNFORD, C.L., in Proc. of Int. Conf. on Nuclear Data for Science and Technology, Jülich, 1991, Springer-Verlag, Berlin (1992) 788.
- [5] NORDBORG, C., SALVATORES, M., in Proc. of Int. Conf. on Nuclear Data for Science and Technology, Gatlinburg, Tennessee, USA, 9-13 May 1993 (1994) 680.
- [6] Japanese Evaluated Data Library, Version 3, Report JAERI-1319 (1990).
- [7] WESTON, L.W., GWIN, R., DE SAUSSURE, G., et al., Nucl. Sci. Eng. **42** (1970) 143.
- [8] KOLAR, W., CARRARO, G., NASTRI, G., in Proc. of Int. Conf. on Nuclear Data for Reactors, Helsinki (1970) 387.
- [9] DERUYTTER, A.J., WAGEMANS, C., Nucl. Sci. Eng. **54** (1974) 423.
- [10] NIZAMUDDIN, S., BLONS, J., Nucl. Sci. Eng. **54** (1974) 116.
- [11] WESTON, L.W., GWIN, R., DE SAUSSURE, G., et al., Nucl. Sci. Eng. **34** (1968) 1.
- [12] MUGHABGHAB, S.F., Neutron Cross Sections, Report BNL-325 (1984), V. 1.
- [13] DUNFORD, C.L., ENDF Utility Codes, Release 6.9, Report INDC(NDS)-29, IAEA, Vienna (1993).

99-11877 (90)

Translated from Russian

UDC 539.163

SERIYA: JADERNYE KONSTANTY, Vypusk 1, 1999, s. 19  
(Series: Nuclear Constants, Issue No. 1 1999, p. 19)

## **RESOLVED RESONANCE PARAMETERS FOR $^{238}\text{Np}$**

G.B. Morogovskij

Institute for Radiation Physics and Chemistry Problems  
National Academy of Sciences, Republic of Belarus

### **ABSTRACT**

Multilevel Breit-Wigner parameters have been obtained for the representation of fission cross-section in the energy region 0.01-6.7 eV on the basis of an evaluation of  $^{238}\text{Np}$  experimental data in the resolved resonance region.

Solving transmutation problems calls for a knowledge of the nuclear physics constants of the actinides in the thermal and resonance neutron range, in particular for the short-lived nucleus  $^{238}\text{Np}$  ( $T_{1/2} = 2.117$  d). Currently there exist four files of evaluated nuclear data on  $^{238}\text{Np}$  [1-4] which are worth closer examination.

At the time when files [1-3] were compiled, no experimental data existed on the cross-sections in the resolved resonance region except for the measurements of  $\sigma_f$  in the thermal point and of the resonance fission integral given in Ref. [5]; the cross-sections for the resolved resonance region in the present evaluations have therefore been based on theoretical considerations taking into account the following quantities from Ref. [5]:  $\sigma_f^{2200} = 2070 \pm 30$  b,  $I_f = 880$  b.

In the ENDF/B-VI file [1]  $\sigma_f^{2200} = 2026.90$  b  $I_f = 898.14$  b, which is close to the corresponding values from Ref. [5]. The upper limit to the resolved resonance region was taken to lie at 100.2 eV. The cross-sections in the resonance region are described by a model set of 94 equidistant resonances in the range 1.517-99.17 eV having identical values of  $\Gamma_n^0$ ,  $\Gamma_f$ ,  $\Gamma_\gamma$  and  $D = 1.05$  eV, together with a negative resonance with an energy  $E_r = -2.03$  eV for the same width  $\Gamma_\gamma$  though with a reduced neutron width 40 times greater than the value of  $\Gamma_n^0$  for the remaining resonances. The fission width of the negative resonances is 12% greater than  $\Gamma_f$  for the other resonances. Obviously the negative resonance is just a construct needed to obtain the required values of  $\sigma_f^{2200}$  and the resonance fission integral.

The JEF-2 file [2] used the same model set as the ENDF/B-VI file, but the values of  $\Gamma_n$  were recalculated because all resonances had been assigned specific spin values of 1.5 or 2.5,

unlike Ref. [1], with  $J = 2$  for all resonances. The result was a value of  $\sigma_f^{2200}$  that was practically the same as in Ref. [1], whereas the resonance fission integral  $I_f = 920.36$  b, owing largely to the difference in the course of  $\sigma_f(E)$  above 10 keV in evaluations [1] and [2].

In the JENDL-3.2 file [3] there are no resonance parameters and the cross-sections are given in terms of a flow representation with an energy dependence  $1/\sqrt{E}$ , which gives values of  $\sigma_f^{2200} = 2070$  b, as in Ref. [5], and  $I_f = 940.58$  b, which is a little more than in Ref. [5].

As file [4] was produced after the publication of Refs. [6-8], it uses a “complex” approach to describe the resonance region: in the energy range 1.2-100 eV the mean resonance parameters  $\langle\Gamma_n^0\rangle$ ,  $\langle\Gamma_P\rangle$ ,  $\langle\Gamma_\gamma\rangle$ ,  $\langle D \rangle$  and  $S^0$  evaluated in the high-energy region served as a basis for generating a set of resonances which, in conjunction with recalculated resonance parameters for energies of -5 eV and 1.14 eV from Ref. [6], was used to obtain values of  $\sigma_f^{2200} = 2075$  b (mean weighted value based on Refs. [5, 7]) and  $I_f = 905$  b [7]. However, such an approach to the representation of evaluated cross-sections in the low-energy region is not entirely correct for the following reasons:

- (1) The information given in the work of Danon et al. [8] leads to the conclusion that the dependence  $\sigma_f(E)$  for the model set of parameters is not the same as the experimentally measured dependence;
- (2) Since the main contribution to the cross-section in the thermal point is from a negative resonance having an enormously large value of  $\Gamma_n^0$  (three orders of magnitude greater than  $\langle\Gamma_n^0\rangle$  for the other resonances), the value  $\sigma_n^{2200}$  is also clearly over-estimated ( $\sigma_n^{2200} = 95.1$  b).

The mean resonance parameters, thermal cross-sections and resonance integrals of the evaluations reviewed are given in Table I.

As already noted above, Ref. [5] was until recently the only paper in which measurements of  $\sigma_f^{2200}$  and  $I_f$  had been carried out, and these served as the basis for files [1-3]. However, in recent years papers by Abramovich et al. [7] and Danon et al. [8] have appeared with measurements of  $\sigma_f^{2200}$  and  $I_f$ , and in addition Ref. [8] contained a measurement of the fission cross-section for the range 0.01-100 eV. The values of  $\sigma_f^{2200} = 2641 \pm 58$  b and  $I_f = 1379 \pm 30$  b given by the authors of Ref. [8] are substantially higher than those from Refs [5, 7], and the measurements of  $\sigma_f^{2200}$  and  $I_f$  for  $^{232}\text{Pa}$  and  $^{236}\text{Np}$  in [8] are also significantly higher than earlier ones. The authors of Ref. [8] were not able to identify the reasons for this discrepancy, but the information on the fission cross-section available from Ref. [8] and the measured values of  $\sigma_f^{2200}$  and  $I_f$  in Refs. [5, 7] are sufficient for an attempt to obtain a set of Breit-Wigner resonance parameters, at least in the low-energy region.

Taking as our basis the measurements  $\sigma_f^{2200} = 2070 \pm 30$  b and  $I_f = 880$  b [5], and also  $\sigma_f^{2200} = 2110 \pm 74$  b and  $I_f = 905 \pm 48$  b [7], we obtain mean-weighted values of  $\sigma_f^{2200} = 2075.65 \pm 27.80$  b and  $I_f \approx 900$  b, with the coefficient for renormalization of the measurements of [8] to the thermal point being 0.7859. Analysis of the experimental values of  $\sigma_f(E)$  gives grounds for hoping to obtain resonance parameters for  $^{238}\text{Np}$  at least up to 6.7 eV.

At the same time it must be noted that the  $^{239}\text{Pu}$  impurity in the sample was not accounted for entirely correctly. The sharp troughs in  $\sigma_f(E)$  at energies of 0.31, 8.0, 11.0, and 17.8 eV and further, in conjunction with the rises in the cross-section curve to the left of the troughs, suggest that the energy scale of the experiment is not commensurate with the  $^{239}\text{Pu}$  resonance energy values used in calculating the impurity. Besides, there is reason to believe that the amount of the  $^{239}\text{Pu}$  impurity in the sample was smaller than the authors assumed.

The data given in Ref. [8] on  $\sigma_f(E)$  for  $^{238}\text{Np}$  allow one fairly confidently to distinguish 15 resonances in the energy range 0.7-6.7 eV. The energy values of these resonances were subsequently determined more precisely, and in addition the behaviour of  $\sigma_f(E)$  in the range 2.5-3.3 eV suggests that there is a fairly broad resonance at an energy of 2.9 eV. The experimental values of  $\sigma_f(E)$  for  $^{238}\text{Np}$  were used to obtain resonance parameters taking into account the resolution function given in Ref. [8] and the renormalization coefficient cited above.

Since the resonance parameters were calculated only on the basis of the fission cross-section there is a fairly large uncertainty in obtaining values of  $\Gamma_\gamma$  for each resonance, for which reason the value  $\langle\Gamma_\gamma\rangle \approx 50$  meV was used as supplementary information.

The measured values of  $\sigma_f(E)$  in Ref. [8] do not allow parametrization in the region above 6.7 eV because of the low energy resolution of the experiment and because above 7 eV an error starts to appear in the description of the  $^{239}\text{Pu}$  impurity which cannot be evaluated accurately on the basis of the information available in Ref. [8].

In the course of the parametrization, the values of the resonance energies were determined more accurately and the values of  $\Gamma_n$ ,  $\Gamma_f$  and  $\Gamma_\gamma$  were obtained for each of them taking into account the assigned resonance spin values.

The contribution to  $\sigma_f^{2200}$  from all resonances above 1 eV is less than 10% of the value of  $\sigma_f^{2200} = 2075.65$  b adopted by us, and consequently we may expect there to be at least one further resonance with an energy of less than 0.5 eV which is needed to obtain the required value of  $\sigma_f^{2200}$ . Test calculations show that the attempt to assign it a negative energy leads either to non-physical values of  $\Gamma_f$  and  $\Gamma_\gamma$ , or to an anomalously large value of  $\Gamma_n$  and, as a result,  $\sigma_n^{2200}$  (see discussion of Ref. [4] above). Solving the problem by obtaining the required

value of  $\sigma_f^{2200}$  and reproducing the course of  $\sigma_f(E)$  in [8] yields a broad resonance with an energy of 0.181 eV and fully physical values of the parameters.

The resonance parameters obtained together with the renormalization coefficient adopted adequately reproduce the course of  $\sigma_f(E)$  from Ref. [8] in the energy range 0.01-6.7 eV. The fission cross-section calculated from the average resonance parameters of the present work also agree well with the course of  $\sigma_f(E)$  in the range 6.7-100 eV as given in Ref. [8].

The value  $I_f = 844.94$  b calculated from the parameters for the range 0.5-6.7 eV is somewhat over-estimated, although it agrees with the values calculated from the experimental fission cross-sections used (with normalization) to an accuracy of 0.8%. However, note that some 60% of this value is attributable to the contribution from the resonance with  $E_\gamma = 1.12$  eV. The final value of  $I_f$  depends heavily on the accuracy of measurement of the course of  $\sigma_f(E)$  in the region of this resonance. It also remains an open question whether there is a resonance at an energy of 3.75 eV, as a satisfactory description of the course of the fission cross-section in this region requires an anomalously small value of  $\Gamma_\gamma$  for this resonance.

The average resonance parameters, thermal cross-sections and resonance integrals from the present work are given in Table I, while Table II shows the resonance parameters obtained in our work. Figure 1 gives the experimental course of the cross-section  $\sigma_f(E)$  in the range 0.01-6.7 eV together with the same course as calculated from the parameters in Table II, and Fig. 2 gives a comparison between the fission cross-sections from evaluations [1-4] and the present work in the same region.

## REFERENCES

- [1] DUNFORD, C.L., Nuclear Data for Science and Technology, Proc. Int. Conf. Jülich, 1991, Springer-Verlag, Berlin (1992), p. 788.
- [2] NORDBORG, C., SALVATORES, M., Nuclear Data for Science and Technology, Proc. of the Int. Conf., Gatlinburg, Tennessee, USA, 9-13 May 1994, V. 2, p. 680.
- [3] Japanese Evaluated Data Library, Version 3, JAERI 1319, 1990.
- [4] MASLOV, V.M., PORODZINSKIJ, Yu.V., SUKHOVITSKIJ, E.Sh., INDC(BLR)-011, IAEA, Vienna (1998).
- [5] SPENCER, J.D., BAUMAN, N.P., Trans. Am. Nucl. Soc. 1969, V. 12, p. 284.
- [6] MOORE, M.S., KOEHLER, P.E., LITTLTON, P.E., et al., Nuclear Data for Science and Technology, Proc. of the Int. Conf., Gatlinburg, Tennessee, USA, 9-13 May 1994, V. 2, p. 1075.
- [7] ABRAMOVICH, S.A., ANDREEV, M., BOL'SHAKOV, Yu., et al., Proc. of the XIII Meeting on Physics of Nuclear Fission in the Memory of SMIRENKO, G.M. (Prof.), Obninsk, 1995, p. 303.
- [8] DANON, Y., MOORE, M.S., KOEHLER, P.E., et al., Nucl. Sci. Eng., 1996, V. 124, p. 482.
- [9] DUNFORD, C.L., ENDF Utility Codes Release 6.9, INDC(NDS)-29, IAEA (1993).

TABLE I. AVERAGE RESONANCE PARAMETERS, THERMAL CROSS-SECTIONS AND RESONANCE INTEGRALS FOR  $^{238}\text{Np}$   
COMPARISON OF EVALUATIONS\*

Quantity	ENDF/B-V1 [1]	JEF-2 [2]	JENDL-3 [3]	Evaluation [4]	Present work
$\langle \Gamma_n^0 \rangle$ , meV	0.2627	0.2903	-	0.5317	0.1010
$\langle \Gamma_\gamma \rangle$ , meV	53.31	53.31	-	50.00	47.95
$\langle \Gamma_f \rangle$ , meV	480.4	480.4	-	654.87	207.16
$\langle D \rangle$ , eV	1.0766	1.0766	-	0.6481	0.4259
$S^0$	$1.233 \times 10^{-4}$	$1.233 \times 10^{-4}$	-	$3.45 \times 10^{-4}$	$1.26 \times 10^{-4}$
R, fm	9.09728	9.09730	-	9.2226	9.2226
$\sigma_t$ , barns	2250.93	2250.45	2532.51	2415.14	2244.22
$\sigma_\gamma$ , barns	202.827	202.824	450.100	257.214	159.66
$\sigma_f$ , barns	2026.85	2026.81	2070.00	2062.82	2075.65
$\sigma_n$ , barns	21.2505	20.8132	12.4095	95.1003	8.9045
$g_\gamma$	0.9941	0.9941	1.00051	1.00032	1.01832
$g_f$	0.99389	0.99389	1.00087	1.00017	1.01707
$I_\gamma$ , barns (0.5-6.7 eV)	69.43	69.42	146.93	87.57	210.31
$I_f$ , barns (0.5-6.7 eV)	650.16	650.08	678.71	694.03	844.94

\* All values in the Table were obtained using the PSYCHE and INTER programs [9].

TABLE II. RESONANCE PARAMETERS FOR  $^{238}\text{Np}$

$E_r$ , eV	J	$\Gamma_n$ , meV	$\Gamma_\gamma$ , meV	$\Gamma_f$ , meV
0.181	1.5	0.13541	58.07	894.431
1.120	2.5	0.28845	51.28	287.980
1.806	1.5	0.16631	52.96	366.510
2.294	2.5	0.10882	38.09	11.295
2.540	2.5	0.07589	40.09	139.740
2.980	1.5	0.18711	52.61	405.360
3.300	2.5	0.11033	47.62	186.310
3.530	1.5	0.15225	46.05	217.970
4.035	2.5	0.15132	42.31	9.050
4.356	2.5	0.10832	45.78	60.517
4.710	2.5	0.12216	44.27	52.623
4.983	1.5	0.12345	51.29	127.060
5.380	2.5	0.09857	42.58	10.567
5.750	2.5	0.08312	44.24	27.756
5.980	1.5	0.30105	57.45	308.930
6.570	2.5	0.23767	52.49	209.350

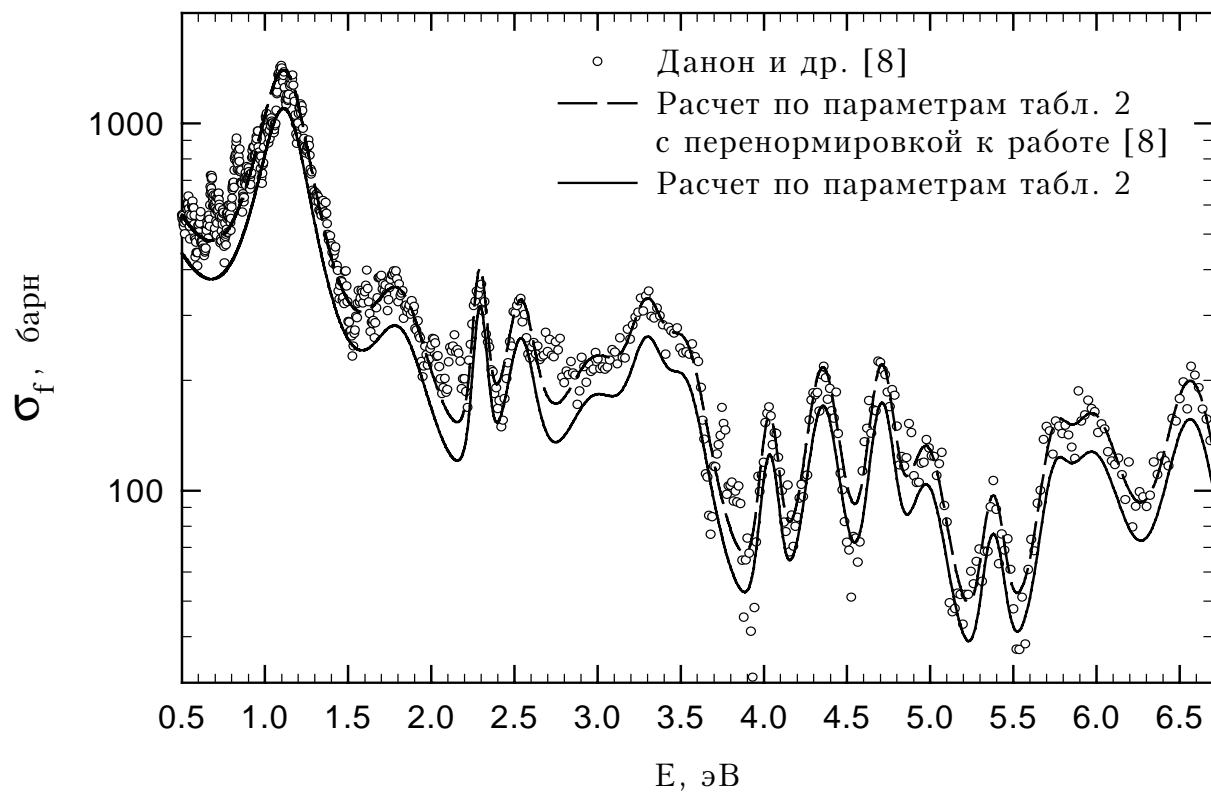
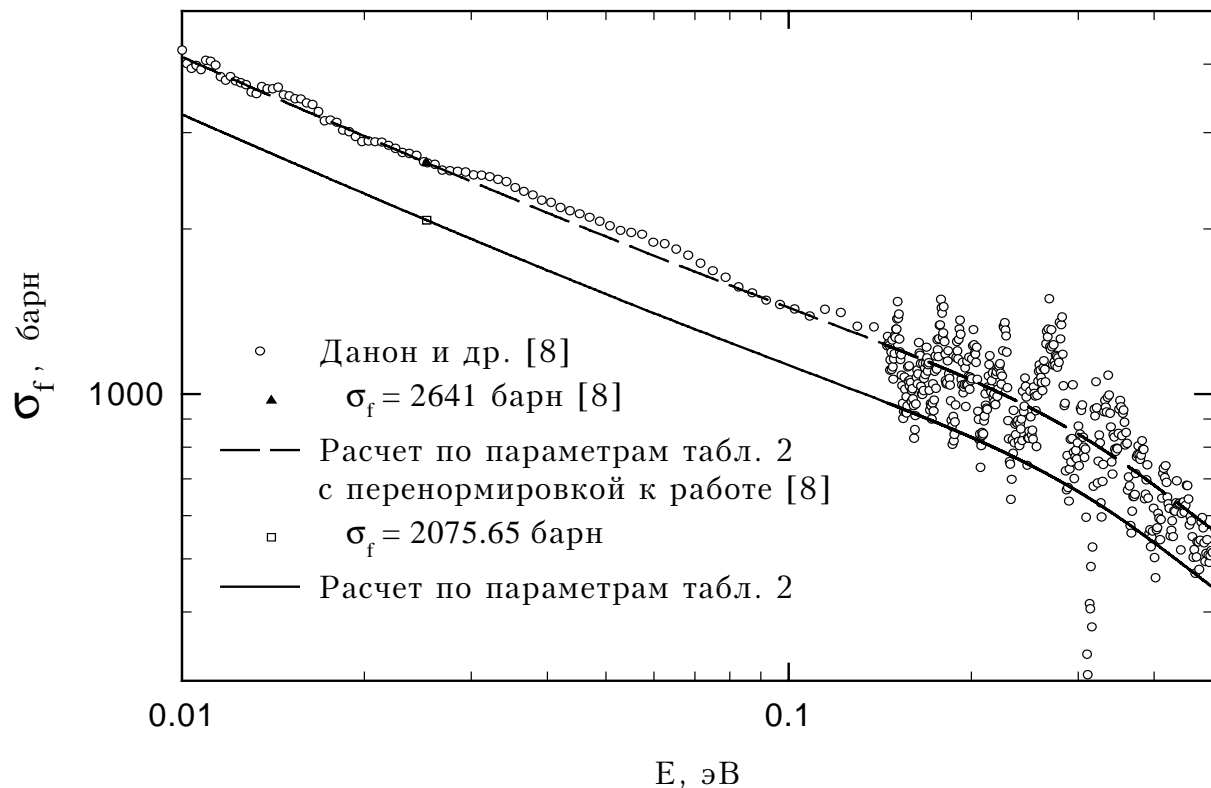


FIG. 1. Comparison of experimental and calculated fission cross sections in the energy range 0.01 – 6.7 eV. Legend: y-axis -  $\sigma_f$ , barns; x – axis – E, eV; open circles – Danon et al. [8]; closed triangle -  $\sigma_f=2641$  barns[8]; dashed line – calculation from parameters of Table II with renormalization to Ref. [8]; open square -  $\sigma_f=2075.65$  barns; solid line – calculations from parameters of Table II.

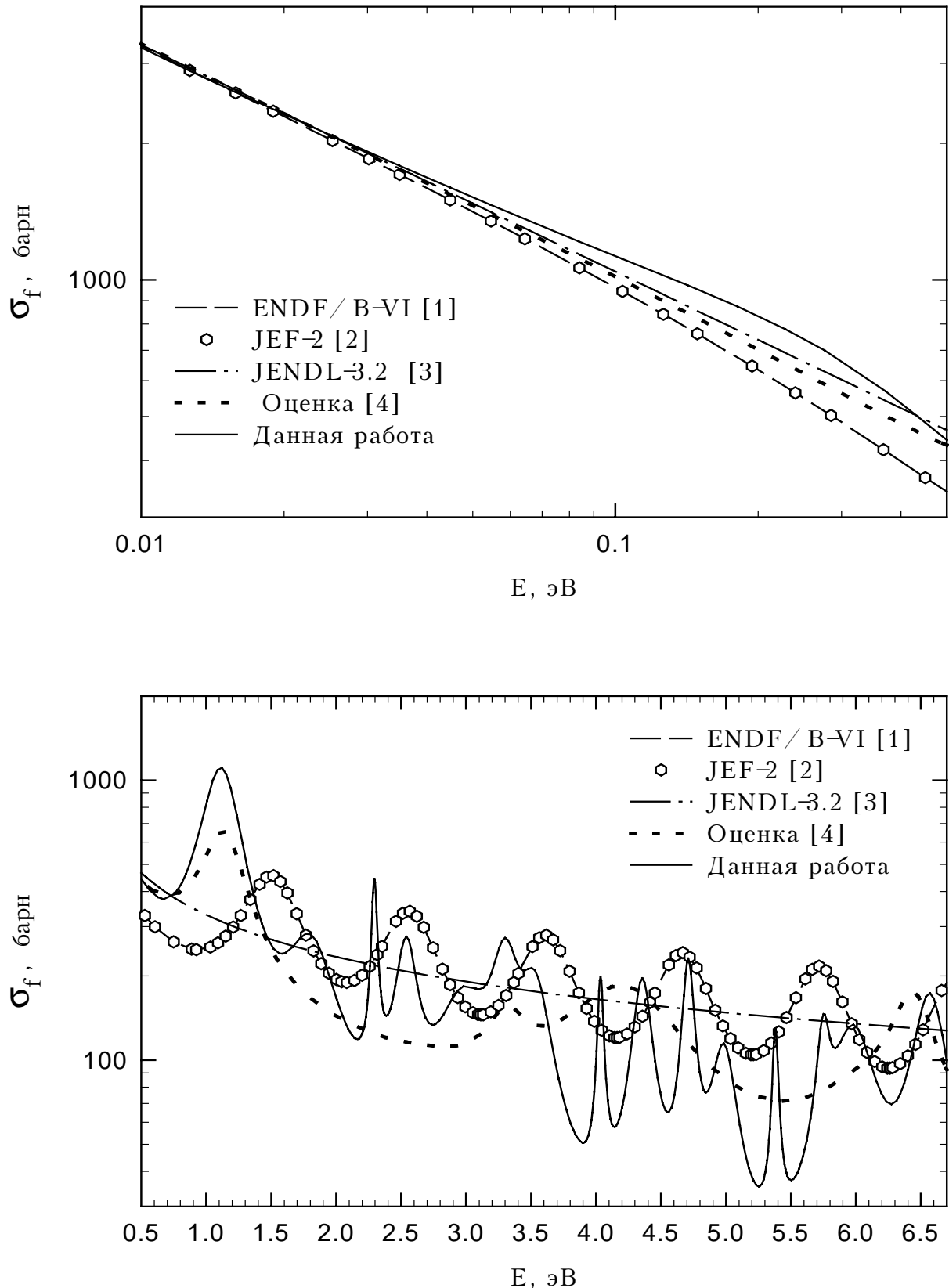


FIG. 2. Comparison of various evaluations of the fission cross section in the energy range 0.01 – 6.7 eV. Cross sections calculated using the RECENT program. Legend: y-axis -  $\sigma_f$ , barns; x – axis – E, eV; dashed line – ENDF/B-VI [1]; open circles – JEF-2 [2]; dot-dashed line – JENDL-3.2 [3]; short dashed line – evaluation [4]; solid line – present work.



99-11877 (90)

Translated from Russian

UDC 539.172

SERIYA: JADERNYE KONSTANTY, Vypusk 1, 1999, s. 42  
(Series: Nuclear Constants, Issue No. 1 1999, p. 42)

## **LEVEL DENSITY PARAMETERS FOR THE BACK-SHIFTED FERMI GAS MODEL IN THE MASS RANGE $24 \leq A \leq 250$**

V.I. Plyaskin and R.A. Kosilov

Institute of Nuclear Power Engineering, Obninsk

### **ABSTRACT**

The parameters  $a$  and  $\delta_{eff}$  for the back-shifted Fermi gas model are determined for 1224 nuclei. For 272 nuclei the parameters are determined from experimental data on cumulative numbers of low-lying levels and the average spacings between neutron resonances. For the rest of the nuclei the  $\delta_{eff}$  parameter was determined from cumulative numbers of low-lying levels and values of the  $a$  parameter obtained by interpolation using the data for the 272 nuclei. A formula is suggested to account for damping of the shell effect at high excitation energies. A comparison is made with previous results and different experimental data on level densities.

### **Introduction**

The Fermi gas model in its various modifications [1-4] is widely used for calculation of the nuclear level density. Despite its fundamental shortcomings [5], this model enables simple systematics to be established based on normalization of the energy dependence of the nuclear level density to data on the cumulative numbers of low-lying levels and the average spacings ( $\bar{D}_0$ ) between S-wave neutron resonances at the neutron binding energy ( $B_n$ ) in the nucleus.

The systematics in Refs [2, 4] are the most widely used. Here it is assumed that both sets of experimental data can be described on the basis of the Fermi gas model relations. However, the level density parameter  $a$  and excitation energy shift  $\delta_{eff}$ , caused by even-odd differences in the nuclei, are considered free parameters. Since the  $\delta_{eff}$  values obtained for odd-odd nuclei are negative, this approximation has been termed the back-shifted Fermi gas model.

All the systematics created within the framework of the back-shifted Fermi gas model [4, 6] contain information about the  $a$  and  $\delta_{eff}$  parameters for approximately 300 nuclei (limited by the volume of experimental data on the average spacings between the S-wave neutron resonances) and have the following drawbacks:

- it is difficult to parametrize the dependence  $\delta_{\text{eff}} = f(A)$ , since it combines in a complex manner the shell and collective effects, and the pairing effects;
- the level density parameter  $a$  does not take account of damping of the shell effects at high nucleus excitation energies.

The systematics proposed give the parameters  $a$  and  $\delta_{\text{eff}}$  for 1224 nuclei, obtained using the method suggested in Ref. [7]. An attempt has been made to provide a phenomenological description of the damping of shell effects in parameter  $a$  as excitation energy increases. The errors in  $a$  and  $\delta_{\text{eff}}$  caused by inaccuracies in the average spacings between the neutron resonances were determined. The effect of the chosen number of low-lying levels on the level density parameters selected was analysed. The parameters  $a$  and  $\delta_{\text{eff}}$  were obtained for two values of the moment of inertia  $F$  of the nucleus:  $F = F_{\text{rig}}$  and  $F = 0.5 \cdot F_{\text{rig}}$  ( $F_{\text{rig}}$  is the rigid body moment of inertia of the nucleus).

Systematics for  $\delta_{\text{eff}} = f(A)$  are proposed which take account of the even-odd effects of the protons and the neutrons in the nuclei. On the basis of the experimental data and the systematics, a database of level density parameters was established for the back-shifted Fermi gas model in the mass range  $24 \leq A \leq 250$  for five thousand nuclei.

### Procedure for obtaining the level density parameters

The procedure used for obtaining the parameters  $a$  and  $\delta_{\text{eff}}$  from experimental data on the cumulative numbers ( $N_0$ ) of the low-lying levels and the average spacings ( $\bar{D}_0$ ) between the S-wave neutron resonances was similar to that proposed in [4].

1. The following expressions were used for the spin-dependent and total level densities:

$$\rho(U, J) = \frac{1}{24\sqrt{2}} \frac{2J+1}{\sigma^3 a^{1/4}} \frac{\exp[2\sqrt{a(U - \delta_{\text{eff}})} - J(J+1)/2\sigma^2]}{(U - \delta_{\text{eff}} + t)^{5/4}}, \quad (1)$$

$$\rho(U) = \frac{1}{12\sqrt{2}} \frac{1}{\sigma a^{1/4}} \frac{\exp[2\sqrt{a(U - \delta_{\text{eff}})}]}{(U - \delta_{\text{eff}} + t)^{5/4}}, \quad (2)$$

where  $U$  is the excitation energy of the nucleus;

$J$  is the total angular momentum;

$a$  is the level density parameter associated with the density of single particle states near the Fermi energy;

$\delta_{\text{eff}}$  is the parameter which fits the back-shifted Fermi gas model;

$t$  is the thermodynamic temperature determined from the expression:

$$U - \delta_{\text{eff}} = at^2 - t, \quad (3)$$

$\sigma$  is the level density spin parameter. In the calculations, the value of  $\sigma_{rig}$  was taken to be

$$\sigma_{rig}^2 = \frac{F_{rig} t}{\hbar^2} \approx 0,015 A^{5/3} t, \quad (4)$$

where  $F_{rig}$  is the rigid body moment of inertia of the nucleus.

2. To obtain the parameters  $a$  and  $\delta_{eff}$ , the following expressions are used:

$$\frac{1}{\overline{D}_0} = \begin{cases} \frac{1}{2} \left( \rho \left( B_n + \frac{1}{2} \Delta E, I_{0+} + \frac{1}{2} \right) + \rho \left( B_n + \frac{1}{2} \Delta E, I_{0+} - \frac{1}{2} \right) \right), & \text{for } I_0 \neq 0 \\ \frac{1}{2} \rho \left( B_n + \frac{1}{2} \Delta E, \frac{1}{2} \right), & \text{for } I_0 = 0 \end{cases}, \quad (5)$$

where upper equation is for  $I_0 \neq 0$  and lower equation is for  $I_0 = 0$ .

$$N_0 = \int_0^{U_0} \rho(U) dU, \quad (6)$$

where  $B_n$  is the neutron binding energy;

$\Delta E$  is the energy range for which resonances were investigated;

$I_0$  is the spin of the target nucleus;

$(\overline{D}_0)$  is the average spacing between the nucleus levels for S-neutrons.

The coefficient 1/2 takes account of the fact that S-neutrons form resonances only at a specific parity;

$N_0$  is the number of low-lying levels of the nucleus under analysis in the excitation energy range from zero to  $U_0$ .

3. The experimental values for  $(\overline{D}_0) \pm \delta(\overline{D}_0)$ ,  $N_0$  and  $U_0$  were taken from Ref. [8]. The  $a$  and  $\delta_{eff}$  parameters were obtained for two values of the moment of inertia of the nucleus:  $F = F_{rig}$  and  $F = 0.5 \cdot F_{rig}$ . Errors in  $a$  and  $\delta_{eff}$  due to inaccuracies in  $(\overline{D}_0)$  were calculated in the following manner. For each nucleus, the  $a$  and  $\delta_{eff}$  parameters were determined using equations (5) and (6) for three values of  $(\overline{D}_0)$ :  $(\overline{D}_0)$ ;  $(\overline{D}_0) \pm \delta(\overline{D}_0)$ ;  $(\overline{D}_0) - \delta(\overline{D}_0)$ . The  $a$  and  $\delta_{eff}$  parameters obtained are shown in Table I. For data were  $F = F_{rig}$  the above errors are given. Fig. 1 shows the averaged values of the parameter  $a$  for  $F = F_{rig}$ .

### Influence of errors in $D_0$ and $N_0$ on the level density parameters

The influence of errors in  $(\overline{D}_0)$  on the values of the level density parameter  $a$  is insignificant and agrees well with the outcome of the elementary analysis of expressions (1, 2) using the theory of errors:

$$\left( \frac{\delta a}{a} \right) = \frac{1}{0.7\sqrt{A}} \frac{\delta \rho(U)}{\rho(U)}.$$

The errors in  $(\bar{D}_0)$  also have an insignificant effect on the absolute values of  $\delta_{eff}$ .

The choice of  $N_0$  and  $U_0$  has a more significant influence on the level density parameters. Table II contains data which can be used to evaluate this influence. The dependence of the  $a$  and  $\delta_{eff}$  values obtained on errors in the calculation of  $N_0$  and on the choice of  $U_0$  is examined for three nuclei from different atomic mass ranges ( $^{63}_{28}$ Ni;  $^{102}_{44}$ Ru;  $^{184}_{74}$ W). The first line for each element gives the  $N_0$  and  $U_0$  used for our calculation. The next two lines give the error levels for  $N_0$ , which are  $\pm 20\%$ . The following lines give the different alternatives for  $N_0$  and  $U_0$  based on an analysis of the level schemes of the nuclides under investigation.

From this example we can conclude that the differences in the level density parameters of the various authors are probably attributable in the main to the choice of the number of low-lying levels  $N_0$  of the nuclide under analysis.

### Dependence of the level density parameter $a$ on the excitation energy

1. Since the Fermi gas level density is obtained for an independent particle model with an equidistant spectrum of single particle levels, it cannot of course describe the effects due to the presence of shells. The presence of a nucleus shell structure causes the level density parameter  $a$  to be dependent on the mass number  $A$ ; this is different from the linear dependence predicted by the Fermi gas model. The shell effects in the level density become weaker as the excitation energy increases and, at relatively high energies ( $\sim 100$  MeV), the dependence of the parameter  $a$  on the mass number approaches the Fermi gas dependence. These features of the behaviour of the level density parameter can be generally substantiated with the help of the shell correction method. The correlation between the shell corrections and the values  $a/A$ , which is clearly evident in the experimental data, is used to construct phenomenological systematics for the change in the level density parameter of the Fermi gas model [9]. These systematics are based on the expression:

$$a(U, Z, A) = \tilde{a}(A) \left\{ 1 + \delta \epsilon_0(Z, A) \frac{f(U)}{U} \right\}, \quad (7)$$

where  $\delta \epsilon_0 = M_{exp}(Z, A) - (Z, A, \beta)$ , which is the shell correction equal to the difference in the experimental value of the mass defect  $M_{exp}$  and its liquid drop component  $M_{ld}$ , calculated for the equilibrium deformation  $\beta$ ;

$\tilde{a}$  is the asymptotic value of the level density parameter at high excitation energies;

$f(U)$  is a dimensionless function determining the energy behaviour of the parameter at low excitation energies. The form of the function:

$$f(U) = 1 - \exp(-\gamma U) \quad (8)$$

is based on an approximation of theoretical calculations of the thermodynamic functions of the nuclei using the shell potential level spectrum [9].

The experimental data in [9] were analysed to obtain the optimum values of the coefficients for this parametrization:  $\tilde{a}/A = 0.154 \text{ MeV}^{-1}$ ,  $\gamma = 0.054 \text{ MeV}$ .

In the course of creating the systematics in Ref. [10] (based on experimental data on neutron resonance density at  $A \geq 150$ ), which take account of the collective increase in the level density of nuclei,  $\tilde{a}/A = 0.0931 \text{ MeV}^{-1}$  and  $\gamma = 0.064 \text{ MeV}$  were also determined; these approximate optimally the correlation between the energy changes in the level density parameters and the shell correction.

Refs [11, 12] showed the need to introduce a weak dependence on the mass number into the parameter  $\gamma$ :

$$\gamma = \gamma_0 A^{-1/3}, \quad (9)$$

where the recommended value of  $\gamma_0 \approx 0.35$ .

2. The shell effects are clearly visible in the parameter  $a$  values obtained by us (Fig. 1), but expression (7) does not take sufficiently accurate account of them. Thus, the following formula was proposed to take account of damping of shell effects as the excitation energy increases:

$$a(U, Z, A) = \tilde{a}(A) \left\{ 1 + \frac{a(B_n, Z, A) - \tilde{a}(A)}{\tilde{a}(A)} \exp[-\gamma_1(U - B_n) \cdot 1(U - B_n)] \right\}, \quad (10)$$

where  $a(B_n, Z, A)$  is the level density parameter obtained in the given systematics;

$B_n$  is the neutron binding energy;

$1(U - B_n)$  is the unit function:

$$1(U - B_n) = \begin{cases} 1, & npu(U - B_n) \geq 0 \\ 0, & npu(U - B_n) < 0 \end{cases}$$

In selecting the parameter  $\gamma_1$ , the best match was taken for the damping rates of the shell effects described by equations (7) and (10). The value adopted was  $\gamma_1 = 0.12A^{-1/3}$ . The asymptotic value of the level density parameter  $\tilde{a}$  we adopted was  $A/9.5$ , with a view to describing the data obtained for nuclei far from shells. This value of  $\tilde{a}$  correlate well with the values calculated in Ref. [13] for the spectrum of single particle states of the Nilsson potential  $-\tilde{a} = (0.105 \pm 0.005)A$  and the Woods-Saxon potential  $-\tilde{a} = (0.090 \pm 0.005)A$ .

3. Equation (10) can be simplified by replacing the binding energy  $B_n$  with 10 MeV, because the influence of damping of shell effects on the level density parameter  $\tilde{a}$  is not significant in the range from  $B_n$  to 10 MeV. In this case, expression (10) takes the form:

$$a(U, Z, A) = \tilde{a}(A) \left\{ 1 + \frac{a(B_n, Z, A) - \tilde{a}(A)}{\tilde{a}(A)} \exp[-\gamma_2(U - 10) \cdot 1(U - 10)] \right\}. \quad (11)$$

In equation (11),  $\gamma_2 = 0.15A^{-1/3}$ .

Fig. 1 shows the values of  $a(U, Z, A)$  at an excitation energy of  $U = 100$  MeV. They agree well with the calculations in Ref. [5], taking into account the discrete shell structure of the single particle levels.

### **Creation of level density parameter systematics for 950 nuclei for which experimental data are available only in low-lying levels**

The shell and collective effects, and the pairing effects combine in a complex manner in the behaviour of the parameter  $\delta_{eff}$  as a function of the atomic mass. The systematics for the parameter  $\delta_{eff}$  in the model under investigation are very problematical, and so this parameter was determined for 952 nuclei, taking the following into consideration: for the majority of the nuclei for which there are no data on the neutron resonance density, experimental information on low levels is available (i.e.  $N_0$  and  $U_0$  are known). The parameter  $\delta_{eff}$  for such nuclei was calculated using the following algorithm: a) the parameter  $a$  was determined by interpolating (details below) between the data calculated using equations (5, 6); b) the parameter  $\delta_{eff}$  was calculated from equation (6).

Using the parameter  $a$  values in Table I, an average dependence  $a(B_n, Z, A) = f(A)$  was obtained for all mass numbers in the range  $24 \leq A \leq 250$ . Expression (7) was used to determine  $a$  for nuclei for which there are no experimental data available on the neutron resonance density. For example, the unknown parameter  $a_l(B_{n1}, Z_1, A)$  for the nucleus  $(Z_1, A)$  is calculated using the formula:

$$a_l(B_{n1}, Z_1, A) = a(B_n, Z, A) \left\{ \frac{1 + K_1 \delta \varepsilon_{01}(Z_1, A)}{1 + K \delta \varepsilon_0(Z, A)} \right\}, \quad (12)$$

where  $a(B_n, Z, A)$  is the level density parameter from the dependence  $a(B_n, Z, A) = f(A)$  (see Fig. 1);

$\delta \varepsilon_{01}(Z_1, A)$ ,  $\delta \varepsilon_0(Z, A)$  are the shell corrections for the nuclei  $(Z_1, A)$  and  $(Z, A)$  respectively;

$K_1 = \{1 - \exp(-\gamma B_{n1})\}/B_{n1}$ ;  $K = \{1 - \exp(-\gamma B_n)\}/B_n$  are coefficients which take account of the energy behaviour of the parameter  $a$  at low excitation energies. Here, it was assumed that  $\gamma = 0.064 \text{ MeV}^{-1}$ ;

$B_{n1}, B_n$  are the neutron binding energies in the nuclei  $(Z_1, A)$  and  $(Z, A)$  respectively.

### **Creation of level density parameter systematics for nuclei for which no experimental data are available**

For some applications (for example, in astrophysics), we need to know the level density parameters of a large number of nuclei for which no experimental data are available either on low-lying levels or for the neutron resonance density. The systematics for the averaged

$\delta_{eff}$  parameters shown in Fig. 2 were created to obtain information on the level density parameters of these nuclei.

By determining  $\delta_{eff}$  for more than 1200 nuclei for which experimental data on low-lying levels are available,  $\delta_{eff} = f(A)$  dependences averaged over a large number of nuclei could be obtained for even-even, even-odd, odd-even and odd-odd nuclides.

The algorithm for obtaining the level density parameters for this group of nuclei was as follows:

- a) The parameters  $a_1(B_{n1}, Z_1, A)$  for the nucleus  $(Z_1, A)$  were determined using a method similar to that described in the previous section using equation (12);
- b) The parameter  $\delta_{eff}$  was determined using one of the  $\delta_{eff} = f(A)$  dependences for a specific mass number  $A$ , taking into account the even-odd effects of the protons and neutrons in this nucleus.

### **Creation of a level density parameter database for the back-shifted Fermi gas model in the mass range $24 \leq A \leq 250$**

Using the level density parameters  $(a, \delta_{eff})$  obtained using the algorithms described above, a database was created for five thousand nuclei. All the level density parameters included in this database can be divided into three types:

1. Those where the parameters  $a$  and  $\delta_{eff}$  were obtained using experimental data on low-lying levels and neutron resonance densities (272 nuclei);
2. Those where the parameters  $a$  were obtained from the averaged dependence  $a(B_n, Z, A) = f(A)$  using equation (12); and where the parameters  $\delta_{eff}$  were determined using experimental data on low-lying levels (950 nuclei);
3. Those where the parameters  $a$  and  $\delta_{eff}$  were determined using the averaged dependences  $a(B_n, Z, A) = f(A)$  using equation (12) and  $\delta_{eff} = f(A)$ , taking into account even-odd effects of the protons and neutrons in the nucleus (all the remaining nuclei).

It should be noted that the type 1 and 2 parameters are of course more accurate than the type 3 parameters.

### **Comparison with the results of other authors**

The parameters we obtained were compared with the corresponding data in Refs [4, 6]. Fig. 3 shows the dependence  $a/a_D = f(A)$ , where  $a/a_D$  is the ratio of the average values of the parameter  $a$  from this paper and from Ref. [6] to the same parameter in Ref. [4].

The spread of the data from the various authors is probably due to the current level of knowledge in this area. The greatest discrepancies ( $\sim 25\%$ ) are observed in the  $A = 60$  region.

Thus, the level density  $\rho(U)$  was calculated for  $^{55}\text{Mn}$  and  $^{60}\text{Co}$  up to higher excitation energies than the neutron binding energies in the corresponding nuclides. The calculation results are shown in Figs 4 and 5. The data in Ref. [6] are lower than the experimental data and level densities calculated using our parameters and the parameters in Ref. [4].

It should be noted that, for  $^{55}\text{Mn}$  and  $^{56}\text{Fe}$  (Fig. 6), the level density was calculated using averaged  $a$  and  $\delta_{\text{eff}}$  values derived for the cumulative numbers of low-lying levels from equation (6). In both cases the calculations agree well with the experimental data.

## Conclusion

The level density parameters  $a$  and  $\delta_{\text{eff}}$  of the back-shifted Fermi gas model were obtained for 272 nuclides using the up-to-date evaluated data in Ref. [8] on the cumulative numbers of low-lying levels and the average spacings between S-wave neutron resonances. Then, for interpolated values of  $a$ , using the cumulative numbers, the  $\delta_{\text{eff}}$  parameters were derived for a further 952 nuclei. In this way, a database of level density parameters was created for 1224 nuclides suitable for a wide variety of applications where a description of the compound nucleus formation and decay processes is required.

A formula was obtained which takes account of the damping of shell effects in the parameter  $a$ , and satisfactorily approximates the well-known expression in Ref. [9].

Systematics for  $\delta_{\text{eff}} = f(A)$  were proposed which take account of the even-odd effects of protons and neutrons in the nuclei. On the basis of the experimental data and the systematics, a database of level density parameters was created for the back-shifted Fermi gas model in the mass range  $24 \leq A \leq 250$  for five thousand nuclei.

The authors will make this level density parameter database and the level density computer program available to all interested parties.

TABLE I. THE LEVEL DENSITY PARAMETERS  $a$  (MeV $^{-1}$ ) AND  $\delta_{eff}$ (MeV),  $\Delta a$  (MeV $^{-1}$ ) AND  $\Delta \delta_{eff}$ (MeV) – ERRORS IN  $a$  AND  $\delta_{eff}$  CAUSED BY ERRORS IN THE AVERAGE SPACINGS ( $\bar{D}_0$ ) BETWEEN THE NUCLEUS LEVELS FOR S-RESONANCES

Z	Sym	A	$F=F_{rig}$				$F=0.5F_{rig}$	
			$a$	$\Delta a$	$\delta$	$\Delta \delta$	$a$	$\delta$
11	Na	24	2.85	0.33	-3.76	0.76	2.44	-4.26
12	Mg	25	2.94	0.37	-1.79	0.86	2.25	-3.43
13	Al	28	3.45	0.50	-2.47	0.98	3.22	-2.39
14	Si	29	4.26	0.46	1.60	0.48	3.40	0.87
16	S	33	3.90	0.26	-0.59	0.34	3.20	-1.24
16	S	34	2.14	0.31	-4.27	1.46	1.73	-6.00
16	S	35	4.54	0.51	0.01	0.43	3.69	-0.52
17	Cl	36	4.20	0.33	-1.47	0.47	3.58	-2.03
17	Cl	38	5.97	0.39	-0.59	0.18	5.29	-0.64
18	Ar	41	5.99	0.38	-0.25	0.21	4.98	-0.60
19	K	40	4.75	0.51	-1.80	0.63	4.03	-2.45
19	K	42	3.99	0.47	-3.88	0.67	3.42	-4.39
20	Ca	41	5.60	0.17	0.06	0.13	4.71	-0.39
20	Ca	43	6.05	0.15	-0.78	0.09	5.22	-0.98
20	Ca	44	5.33	0.66	0.20	0.64	5.11	0.38
20	Ca	45	6.40	0.20	-0.14	0.13	5.36	-0.62
21	Sc	46	5.97	0.09	-2.14	0.08	5.72	-1.99
22	Ti	47	4.98	0.19	-2.16	0.22	4.23	-2.72
22	Ti	48	5.46	0.15	-0.27	0.15	4.96	-0.39
22	Ti	49	6.73	0.24	0.44	0.15	5.68	0.01
22	Ti	50	6.02	0.30	1.79	0.24	5.71	1.89
22	Ti	51	5.84	1.20	-0.18	0.66	4.80	-0.65
23	V	51	5.85	0.31	-0.04	0.19	6.45	0.59
23	V	52	6.48	0.23	-1.05	0.16	6.16	-0.94
24	Cr	51	5.90	0.10	-0.76	0.07	5.11	-1.04
24	Cr	53	5.73	0.12	-0.65	0.08	4.88	-0.96
24	Cr	54	5.67	0.12	0.16	0.11	4.90	-0.22
24	Cr	55	6.55	0.22	-0.41	0.14	5.39	-0.95
25	Mn	56	6.00	0.21	-3.26	0.18	5.39	-3.45
26	Fe	55	5.77	0.15	-0.85	0.12	4.96	-1.23
26	Fe	57	6.16	0.12	-1.18	0.11	5.16	-1.80
26	Fe	58	6.18	0.20	0.06	0.17	5.30	-0.40
26	Fe	59	7.82	0.38	0.25	0.18	6.52	-0.20
27	Co	60	7.15	0.17	-1.77	0.11	6.68	-1.74
28	Ni	59	6.22	0.08	-0.88	0.07	5.30	-1.39
28	Ni	60	6.07	0.44	0.05	0.34	5.36	-0.22
28	Ni	61	7.16	0.10	-0.34	0.07	6.06	-0.82
28	Ni	62	6.52	0.08	0.27	0.06	5.74	0.01
28	Ni	63	8.87	0.40	0.92	0.16	7.45	0.54
28	Ni	65	8.77	0.29	0.22	0.09	7.46	-0.03
29	Cu	64	7.48	0.14	-1.78	0.09	6.59	-2.08
29	Cu	66	7.96	0.11	-1.59	0.05	7.06	-1.75
30	Zn	65	8.07	0.06	-0.82	0.03	7.04	-1.07
30	Zn	67	8.51	0.18	-0.90	0.07	7.40	-1.14
30	Zn	68	8.25	0.18	0.67	0.06	7.54	0.67
30	Zn	69	8.91	0.11	-0.84	0.04	7.79	-1.00
30	Zn	71	9.50	0.18	-0.66	0.05	8.30	-0.77
31	Ga	70	8.99	0.25	-1.43	0.09	8.06	-1.55
31	Ga	72	9.01	0.24	-2.51	0.09	8.04	-2.68

Z	Sym	A	$F=F_{rig}$				$F=0.5F_{rig}$	
			$a$	$\Delta a$	$\delta$	$\Delta\delta$	$a$	$\delta$
32	Ge	71	9.81	0.44	-1.11	0.14	8.70	-1.26
32	Ge	73	10.08	0.52	-1.38	0.14	8.93	-1.53
32	Ge	74	10.15	0.41	0.80	0.14	9.82	0.92
32	Ge	75	9.56	0.62	-1.05	0.19	8.37	-1.24
32	Ge	77	9.33	0.59	-1.35	0.16	8.18	-1.49
33	As	76	10.32	0.15	-2.15	0.05	9.33	-2.26
34	Se	75	10.21	0.35	-1.32	0.10	9.14	-1.44
34	Se	77	10.30	0.23	-1.15	0.06	9.18	-1.26
34	Se	78	10.33	0.42	0.65	0.12	9.30	0.53
34	Se	79	9.28	0.40	-1.55	0.14	8.18	-1.73
34	Se	81	10.29	0.74	-0.76	0.15	9.13	-0.84
34	Se	83	10.54	1.14	-0.52	0.22	9.25	-0.62
35	Br	80	10.62	0.15	-1.95	0.04	9.64	-2.04
35	Br	82	10.71	0.21	-1.29	0.05	9.68	-1.37
36	Kr	79	10.26	0.49	-1.44	0.14	9.22	-1.55
36	Kr	81	11.30	0.37	-0.84	0.07	10.19	-0.88
36	Kr	84	8.97	0.89	0.82	0.28	8.48	0.89
36	Kr	85	14.23	0.93	1.08	0.12	12.68	1.00
37	Rb	86	9.38	0.24	-1.03	0.08	8.55	-1.07
37	Rb	88	10.28	0.31	-0.34	0.08	9.07	-0.47
38	Sr	85	11.12	0.67	-0.23	0.15	9.97	-0.32
38	Sr	87	9.46	0.49	0.16	0.13	8.39	0.06
38	Sr	88	9.05	0.43	1.88	0.15	8.51	1.92
38	Sr	89	10.59	0.63	1.51	0.18	8.76	1.10
39	Y	90	9.02	0.16	-0.80	0.05	7.94	-0.92
40	Zr	91	10.19	0.45	0.50	0.13	8.86	0.29
40	Zr	92	9.88	0.29	0.77	0.08	8.92	0.71
40	Zr	93	10.56	0.39	-0.24	0.08	9.34	-0.32
40	Zr	94	12.17	0.16	1.09	0.03	11.13	1.09
40	Zr	95	11.76	0.48	0.31	0.07	10.41	0.26
40	Zr	97	11.85	0.52	0.69	0.08	10.30	0.60
41	Nb	94	11.30	0.21	-1.12	0.05	10.71	-1.07
42	Mo	93	9.71	0.32	-0.06	0.11	8.50	-0.31
42	Mo	95	10.78	0.22	-0.48	0.05	9.59	-0.60
42	Mo	96	10.96	0.13	0.48	0.03	10.03	0.47
42	Mo	97	11.84	0.36	-0.38	0.08	10.49	-0.52
42	Mo	98	12.31	0.52	0.81	0.11	11.22	0.74
42	Mo	99	12.53	0.38	-0.84	0.07	11.14	-0.93
42	Mo	101	12.68	0.36	-1.51	0.07	11.27	-1.63
43	Tc	100	14.10	0.25	-1.22	0.03	13.47	-1.15
44	Ru	100	12.13	0.23	0.52	0.03	11.19	0.54
44	Ru	102	13.65	0.29	1.00	0.05	12.56	0.97
44	Ru	103	12.23	0.50	-1.43	0.10	10.94	-1.52
44	Ru	105	13.44	0.49	-1.44	0.08	12.06	-1.52
45	Rh	104	13.82	0.21	-1.49	0.03	12.56	-1.55
46	Pd	106	13.86	0.08	0.89	0.02	12.76	0.86
46	Pd	107	13.06	0.64	-1.24	0.10	11.76	-1.30
46	Pd	108	14.36	0.13	0.95	0.02	13.26	0.95
46	Pd	109	15.25	0.44	-1.13	0.06	13.81	-1.18
46	Pd	111	15.94	0.77	-0.76	0.08	14.39	-0.80
47	Ag	108	14.36	0.31	-1.25	0.05	13.08	-1.29
47	Ag	110	15.60	0.16	-1.22	0.02	14.23	-1.26
48	Cd	107	13.08	0.45	-0.50	0.07	11.85	-0.55
48	Cd	109	14.19	0.46	-0.41	0.06	12.85	-0.45

Z	Sym	A	$F=F_{rig}$				$F=0.5F_{rig}$	
			$a$	$\Delta a$	$\delta$	$\Delta\delta$	$a$	$\delta$
48	Cd	111	14.19	0.23	-0.57	0.03	12.83	-0.62
48	Cd	112	15.03	0.36	1.20	0.05	13.69	1.15
48	Cd	113	14.54	0.24	-0.63	0.03	13.12	-0.69
48	Cd	114	15.17	0.19	1.09	0.03	13.80	1.03
48	Cd	115	14.51	0.28	-0.91	0.04	13.09	-0.95
48	Cd	117	14.34	0.47	-0.99	0.06	12.88	-1.05
49	In	114	14.25	0.42	-0.80	0.06	13.48	-0.75
49	In	116	15.23	0.09	-0.94	0.01	14.44	-0.89
50	Sn	113	14.34	0.68	0.28	0.10	12.95	0.21
50	Sn	115	14.07	0.74	0.39	0.08	12.73	0.37
50	Sn	117	13.41	0.27	0.00	0.03	12.06	-0.03
50	Sn	118	13.97	0.15	1.16	0.02	12.67	1.11
50	Sn	119	15.81	0.44	0.67	0.05	14.10	0.58
50	Sn	120	13.31	0.37	0.86	0.05	12.08	0.83
50	Sn	121	14.24	0.27	0.48	0.04	12.54	0.34
50	Sn	125	11.33	0.18	-0.36	0.03	9.94	-0.48
51	Sb	124	13.64	0.22	-1.73	0.04	12.59	-1.76
52	Te	123	15.55	0.47	-0.50	0.05	14.14	-0.52
52	Te	124	14.95	0.31	0.79	0.05	13.64	0.74
52	Te	125	14.80	0.19	-0.65	0.02	13.39	-0.69
52	Te	126	14.47	0.22	0.83	0.03	13.15	0.77
52	Te	127	13.61	0.33	-0.82	0.05	12.23	-0.88
52	Te	129	13.90	0.39	-0.60	0.05	12.48	-0.65
52	Te	131	14.46	0.82	0.12	0.11	12.84	0.04
53	I	128	14.11	0.36	-1.70	0.06	12.93	-1.75
53	I	130	12.50	0.17	-2.56	0.05	11.45	-2.66
54	Xe	129	13.71	0.01	-0.88	0.00	12.40	-0.92
54	Xe	130	14.07	0.20	0.60	0.02	12.85	0.59
54	Xe	131	14.90	0.53	-0.47	0.06	13.47	-0.52
54	Xe	132	13.69	0.58	0.81	0.09	12.45	0.76
54	Xe	133	13.86	0.41	-0.37	0.05	12.45	-0.42
55	Cs	134	13.45	0.16	-1.73	0.03	12.40	-1.77
56	Ba	131	15.15	0.30	-0.63	0.04	13.80	-0.66
56	Ba	135	15.28	0.12	-0.24	0.01	13.85	-0.27
56	Ba	136	12.74	0.24	0.49	0.04	11.73	0.47
56	Ba	137	16.78	0.14	1.34	0.02	15.01	1.27
56	Ba	138	12.12	0.31	0.73	0.05	10.95	0.70
56	Ba	139	13.11	0.41	0.09	0.07	11.20	-0.13
57	La	139	12.44	0.29	-0.21	0.05	11.64	-0.17
57	La	140	14.90	0.48	-0.59	0.09	13.47	-0.69
58	Ce	137	16.45	0.87	-0.04	0.08	15.01	-0.06
58	Ce	141	15.59	0.42	0.57	0.05	13.68	0.46
58	Ce	143	18.86	1.72	0.77	0.15	16.64	0.68
59	Pr	142	14.25	0.36	-1.02	0.05	12.94	-1.06
60	Nd	143	15.72	0.19	0.36	0.02	14.11	0.33
60	Nd	144	15.88	0.31	1.10	0.04	14.60	1.07
60	Nd	145	17.97	0.28	0.48	0.03	16.02	0.39
60	Nd	146	16.12	0.33	0.38	0.03	14.95	0.40
60	Nd	147	17.88	0.41	-0.34	0.04	16.09	-0.39
60	Nd	148	19.01	1.22	0.24	0.07	17.61	0.25
60	Nd	149	18.43	0.34	-0.92	0.03	16.66	-0.97
60	Nd	151	18.13	0.30	-0.68	0.03	16.38	-0.73
61	Pm	148	18.87	0.53	-0.84	0.04	17.56	-0.83
62	Sm	145	14.95	0.18	0.37	0.02	13.42	0.32

Z	Sym	A	$F=F_{rig}$				$F=0.5F_{rig}$	
			$a$	$\Delta a$	$\delta$	$\Delta\delta$	$a$	$\delta$
62	Sm	148	17.59	0.19	0.79	0.02	16.34	0.78
62	Sm	149	18.04	0.45	-0.47	0.04	16.37	-0.50
62	Sm	150	19.15	0.30	0.71	0.03	17.85	0.71
62	Sm	151	18.51	0.38	-1.11	0.04	16.84	-1.15
62	Sm	152	19.83	0.30	0.62	0.02	18.39	0.60
62	Sm	153	17.49	0.21	-1.34	0.03	15.90	-1.40
62	Sm	155	18.17	0.29	-0.45	0.03	16.45	-0.50
63	Eu	152	20.62	0.20	-1.22	0.02	19.14	-1.24
63	Eu	153	17.34	0.31	-0.90	0.04	16.16	-0.90
63	Eu	154	19.75	0.39	-1.22	0.04	18.31	-1.23
63	Eu	155	17.30	0.22	-0.92	0.02	16.12	-0.91
63	Eu	156	17.92	0.79	-1.24	0.08	16.52	-1.26
64	Gd	153	19.03	0.45	-1.12	0.04	17.42	-1.15
64	Gd	155	18.89	0.21	-0.99	0.02	17.29	-1.03
64	Gd	156	19.00	0.24	0.55	0.03	17.51	0.51
64	Gd	157	18.23	0.41	-0.88	0.03	16.66	-0.90
64	Gd	158	18.55	0.20	0.50	0.02	17.02	0.46
64	Gd	159	17.18	0.14	-1.09	0.02	15.61	-1.13
64	Gd	161	17.19	0.21	-0.73	0.02	15.57	-0.76
65	Tb	160	18.42	0.13	-1.27	0.02	16.92	-1.31
66	Dy	161	17.76	0.37	-1.16	0.04	16.23	-1.19
66	Dy	162	17.87	0.14	0.07	0.01	16.57	0.08
66	Dy	163	17.33	0.16	-0.94	0.02	15.78	-0.98
66	Dy	164	18.82	0.19	0.78	0.02	17.29	0.75
66	Dy	165	16.95	0.13	-1.03	0.02	15.35	-1.08
67	Ho	166	18.42	0.25	-1.04	0.03	17.08	-1.05
68	Er	163	19.86	0.49	-0.74	0.04	18.27	-0.77
68	Er	165	18.17	0.38	-0.98	0.04	16.64	-1.01
68	Er	167	18.31	0.16	-0.70	0.02	16.70	-0.74
68	Er	168	18.30	0.15	0.41	0.02	16.92	0.38
68	Er	169	17.09	0.19	-1.03	0.02	15.54	-1.07
68	Er	171	17.58	0.29	-0.84	0.03	15.94	-0.88
69	Tm	170	18.65	0.16	-1.01	0.02	17.12	-1.04
69	Tm	171	18.82	0.53	-0.34	0.04	17.33	-0.35
70	Yb	169	17.60	0.45	-1.09	0.05	16.13	-1.11
70	Yb	170	18.34	0.14	0.14	0.01	17.12	0.16
70	Yb	171	17.02	0.08	-0.91	0.01	15.53	-0.94
70	Yb	172	19.57	0.17	0.56	0.02	17.92	0.50
70	Yb	173	17.62	0.07	-0.71	0.01	16.06	-0.74
70	Yb	174	18.35	0.23	0.37	0.01	16.93	0.38
70	Yb	175	18.16	0.23	-0.41	0.02	16.47	-0.43
70	Yb	177	18.00	0.21	-0.66	0.02	16.32	-0.68
71	Lu	176	18.08	0.05	-0.97	0.01	16.73	-0.99
71	Lu	177	18.18	0.68	-0.55	0.06	17.47	-0.49
72	Hf	175	18.72	0.59	-0.87	0.05	17.18	-0.89
72	Hf	177	19.26	0.50	-0.58	0.03	17.64	-0.59
72	Hf	178	19.27	0.24	0.22	0.01	17.94	0.24
72	Hf	179	18.78	0.22	-0.64	0.02	17.14	-0.66
72	Hf	180	18.72	0.14	0.29	0.02	17.46	0.29
72	Hf	181	18.76	0.35	-0.71	0.03	17.08	-0.74
73	Ta	181	20.49	0.32	-0.41	0.02	18.98	-0.40
73	Ta	182	19.32	0.15	-0.94	0.01	17.90	-0.95
73	Ta	183	19.04	0.42	-0.20	0.03	17.89	-0.17
74	W	181	19.23	0.80	-0.63	0.06	17.64	-0.65

Z	Sym	A	$F=F_{rig}$				$F=0.5F_{rig}$	
			$a$	$\Delta a$	$\delta$	$\Delta\delta$	$a$	$\delta$
74	W	183	18.51	0.20	-0.68	0.02	16.88	-0.70
74	W	184	19.61	0.17	0.37	0.01	17.94	0.34
74	W	185	18.84	0.21	-0.87	0.02	17.17	-0.90
74	W	187	19.75	0.21	-0.66	0.02	17.98	-0.68
75	Re	186	20.09	0.20	-0.90	0.02	18.55	-0.91
75	Re	188	20.13	0.16	-1.01	0.01	18.56	-1.03
76	Os	187	19.32	0.21	-0.77	0.02	17.65	-0.80
76	Os	188	19.92	0.28	0.26	0.02	18.39	0.27
76	Os	189	19.22	0.27	-0.86	0.02	17.55	-0.88
76	Os	190	20.44	0.25	0.64	0.02	18.79	0.61
76	Os	191	18.89	0.31	-0.90	0.03	17.19	-0.94
76	Os	193	19.01	0.18	-0.69	0.02	17.29	-0.72
77	Ir	192	20.90	0.45	-0.99	0.03	19.26	-1.00
77	Ir	193	19.21	0.58	-0.66	0.05	17.97	-0.64
77	Ir	194	19.16	0.66	-1.18	0.06	17.57	-1.21
78	Pt	193	19.23	0.85	-0.93	0.07	17.61	-0.95
78	Pt	195	16.42	0.96	-1.03	0.11	14.86	-1.09
78	Pt	196	18.59	0.35	0.58	0.04	16.98	0.54
78	Pt	197	16.06	0.63	-1.06	0.08	14.50	-1.12
78	Pt	199	17.27	0.61	-0.76	0.06	15.61	-0.80
79	Au	198	17.14	0.10	-1.16	0.01	15.67	-1.20
80	Hg	199	17.18	0.73	-0.61	0.07	15.65	-0.64
80	Hg	200	16.12	0.85	0.49	0.11	14.64	0.43
80	Hg	201	13.04	1.17	-1.15	0.19	11.67	-1.24
80	Hg	202	14.85	0.65	0.06	0.07	13.53	0.05
81	Tl	204	14.01	0.32	-1.23	0.05	12.66	-1.29
81	Tl	206	11.06	0.52	-0.89	0.13	9.75	-1.06
82	Pb	205	13.97	0.53	-0.05	0.09	12.47	-0.15
82	Pb	207	11.79	0.36	0.95	0.06	10.35	0.86
82	Pb	208	11.38	0.46	2.07	0.09	9.85	1.92
82	Pb	209	10.31	-	0.23	-	8.47	-0.02
83	Bi	210	10.95	0.36	-1.76	0.09	9.68	-1.93
88	Ra	227	25.05	0.67	-0.85	0.04	22.89	-0.88
90	Th	229	25.93	2.25	-0.87	0.11	23.87	-0.89
90	Th	230	24.77	0.48	0.11	0.02	23.00	0.11
90	Th	231	25.93	0.41	-0.64	0.02	23.83	-0.65
90	Th	233	26.24	0.10	-0.59	0.01	24.05	-0.61
92	U	233	25.63	0.38	-0.53	0.02	23.65	-0.53
92	U	234	26.20	0.23	0.51	0.01	24.28	0.49
92	U	235	24.11	0.16	-0.89	0.01	22.14	-0.91
92	U	236	25.98	0.10	0.13	0.01	24.27	0.14
92	U	237	25.15	0.16	-0.63	0.01	23.10	-0.64
92	U	238	25.74	0.59	0.12	0.02	23.77	0.13
92	U	239	25.81	0.04	-0.60	0.00	23.66	-0.61
93	Np	238	26.67	0.13	-0.71	0.01	24.77	-0.72
94	Pu	239	25.00	0.28	-0.46	0.02	23.00	-0.47
94	Pu	240	25.25	0.05	0.07	0.00	23.36	0.08
94	Pu	241	24.90	0.14	-0.72	0.01	22.89	-0.73
94	Pu	243	26.83	0.30	-0.36	0.01	24.67	-0.37
94	Pu	245	29.50	0.72	0.00	0.02	27.07	0.00
95	Am	242	26.43	0.17	-0.75	0.01	24.54	-0.75
95	Am	243	26.09	0.48	-0.63	0.02	24.24	-0.63
96	Cm	243	22.89	0.53	-0.86	0.03	21.04	-0.88
96	Cm	245	24.95	0.24	-0.48	0.01	22.96	-0.48

Z	Sym	A	$F=F_{rig}$				$F=0.5F_{rig}$	
			$a$	$\Delta a$	$\delta$	$\Delta\delta$	$a$	$\delta$
96	Cm	246	27.03	0.37	0.19	0.01	25.06	0.20
96	Cm	247	23.85	0.44	-0.64	0.02	21.84	-0.66
96	Cm	248	24.66	0.41	0.26	0.02	23.03	0.28
96	Cm	249	25.66	0.50	-0.63	0.02	23.49	-0.64
97	Bk	250	26.28	0.24	-0.91	0.01	24.38	-0.92
98	Cf	250	24.95	0.33	0.19	0.01	23.35	0.21

TABLE II. INFLUENCE OF  $N_0$  AND  $U_0$  ON THE LEVEL DENSITY PARAMETERS  $a$  AND  $\delta_{eff}$

$N_0$	$U_0$ , MeV	$a$ , 1/MeV	$\delta_{eff}$ , MeV	Nuclide
61	4,106	8,87	0,92	
80(+20%)	4,106	8,52	0,57	
41(-20%)	4,106	9,37	1,38	
40	3,52	8,43	0,47	$^{63}_{28}Ni$
28	3,01	8,1	0,09	
20	2,519	7,82	-0,26	
15	2,15	7,64	-0,5	
53	3,086	13,65	1,0	
63(+20%)	3,086	13,51	0,88	
43(-20%)	3,086	13,82	1,12	
27	2,56	13,31	0,73	$^{102}_{44}Ru$
15	2,19	13,16	0,6	
10	1,84	12,9	0,4	
48	1,894	19,61	0,37	
58(+20%)	1,894	19,43	0,29	
38(-20%)	1,894	19,82	0,46	$^{184}_{74}W$
30	1,61	19,27	0,21	
20	1,42	19,12	0,14	
12	1,25	19,09	0,13	

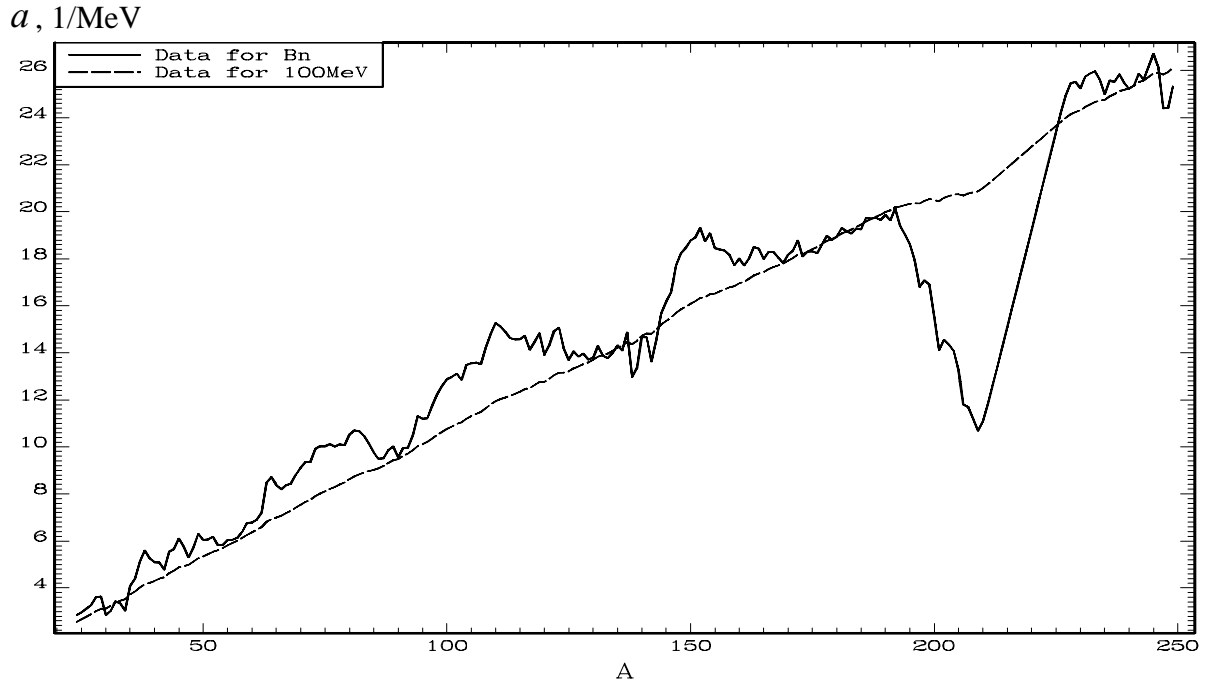


FIG.1. Graph of the dependence of the parameter  $a$  in the mass number. Solid line: averaged values of the parameter  $a$  derived from data on the cumulative numbers of low-lying levels and the density of S-wave neutron resonances. Dashed line: values of the parameter  $a$  at an excitation energy of 100 MeV. Damping of the shell effects was calculated using equation (11).

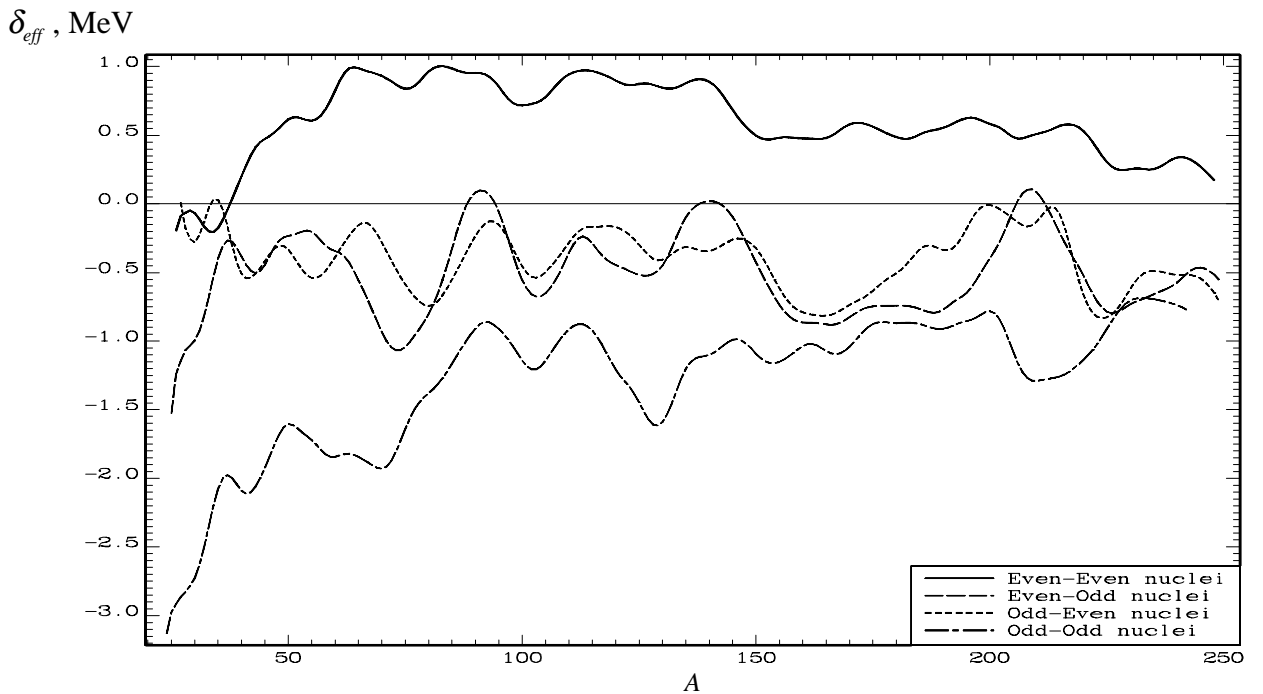


FIG. 2. Graph of the averaged values of the parameter  $\delta_{\text{eff}}$  as a function of the mass number taking into account even-odd effects of protons and neutrons in nuclei.

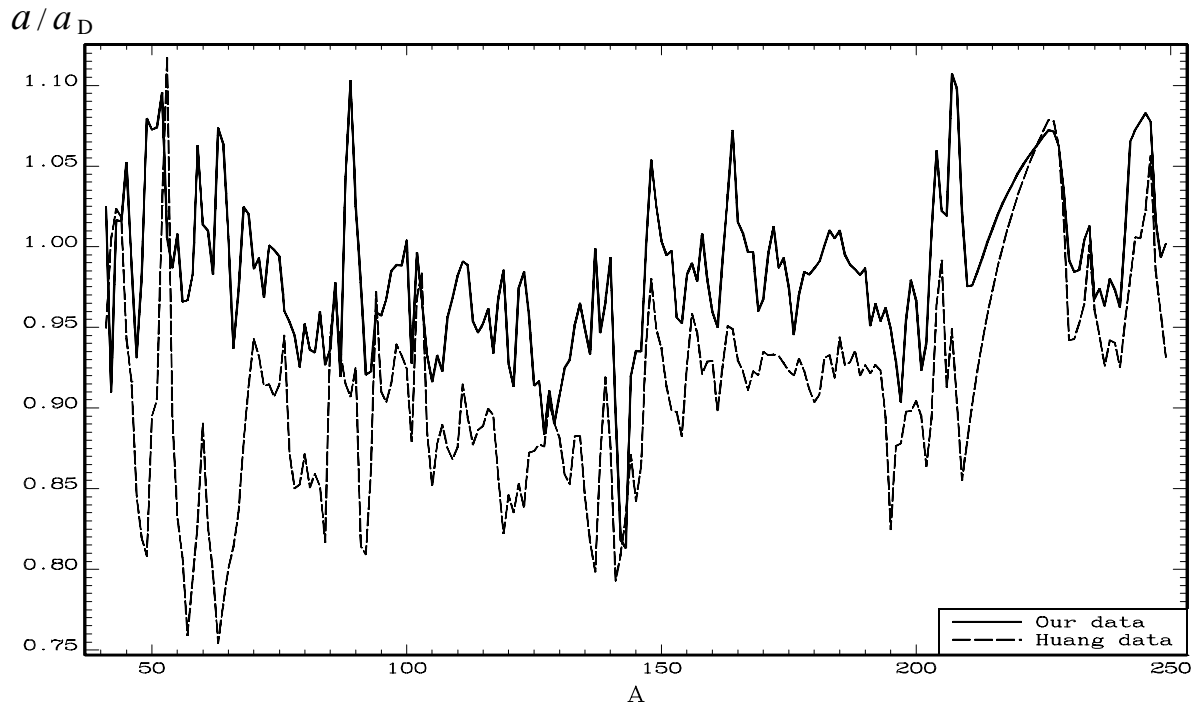


FIG. 3. Graph of the dependence  $a/a_D = f(A)$ .  $a/a_D$  is the ratio of the averaged parameter  $a$  values from this paper and from Ref. [6] to the same parameter in Ref. [4]. Solid line: this paper. Dashed line: Ref. [6].

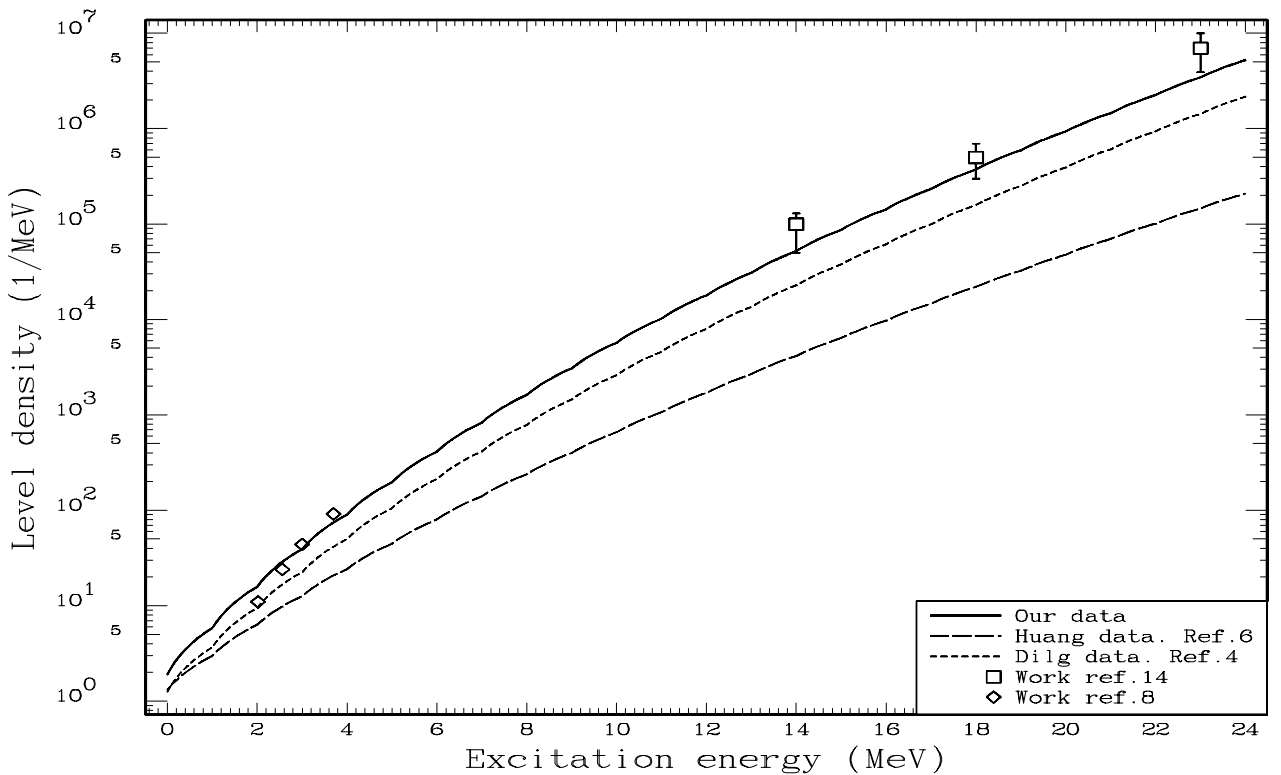


FIG. 4. Comparison of the experimental data and calculated level densities for  $^{55}\text{Mn}$ .

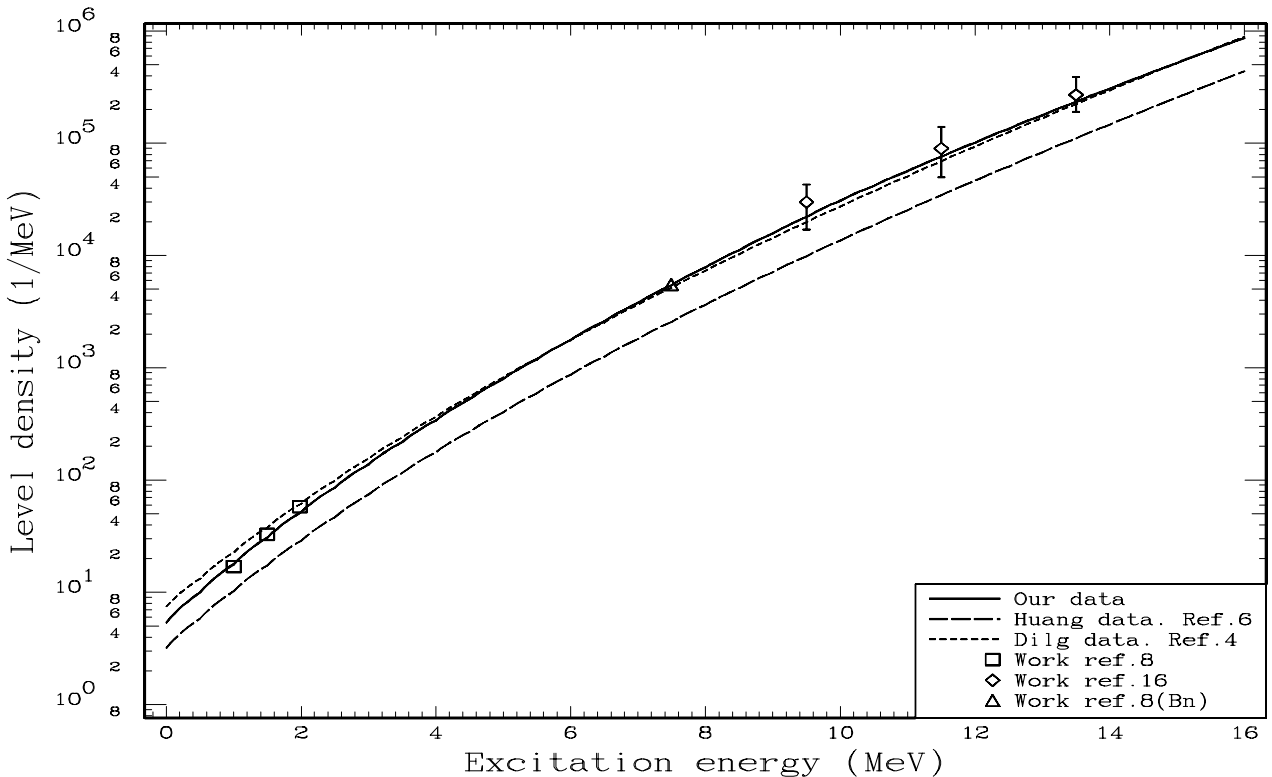


FIG. 5. Comparison of the experimental data and calculated level densities for  $^{60}\text{Co}$ .

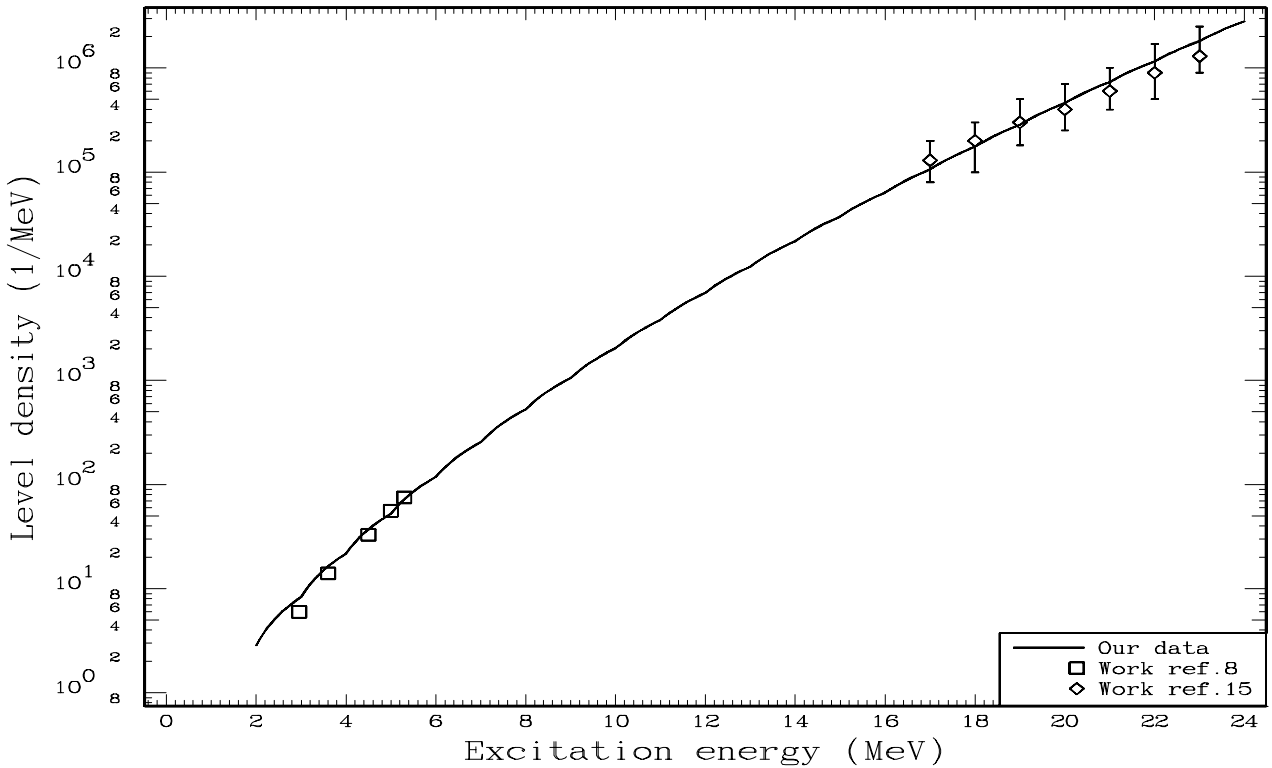


FIG. 6. Comparison of the experimental data with the calculated level density using our parameters for  $^{56}\text{Fe}$ .

## REFERENCES

- [1] GILBERT, A., CAMERON, A.G.W., Can. J. Phys., 1965, v. 43, p.1446.
- [2] VONACH, H.K., HUIZENGA, J.K., Phys. Rev., 1965, v. B138, p. 1372.
- [3] MALYSHEV, A.V., Level Density and Structure of Atomic Nuclei, Atomizdat, Moscow (1965).
- [4] DILG, W., SCHANTL, W., VONACH, H., UHL, M., Nucl. Phys., 1973, v. A217, p. 269.
- [5] IGNATYUK, A.V., Statistical Properties of Excited Atomic Nuclei, Ehnergoatomizdat, Moscow (1983).
- [6] HUANG Zhongfu, HE Ping, SU Zongdi, ZHOU Chunmei, Chin. J. Nucl. Phys., 1991, v. 13, p. 147.
- [7] BYCHKOV, V.M., GRUDZEVICH, O.T., PLYASKIN, V.I., Voprosy Atomnoj Nauki i Tekhniki, Seriya: Jadernye Konstanty 3 (1987) 14.
- [8] Handbook for calculations nuclear reaction data, Report IAEA-TECDOC-1034, Vienna (1998).
- [9] IGNATYUK, A.V., SMIRENKO, G.N., TISHIN, A.S., Jadernaya Fisika **21** (1975) 485.
- [10] IGNATYUK, A.V., ISTEKOV, K.K., SMIRENKO, G.N., Jadernaya Fisika **29** (1979) 875.
- [11] RAMAMURTHY, V.S., KATARIA, S.K., KAPOOR, S.S., In Proc. IAEA Advisory Group Meeting on Basic and Applied Problems of Nuclear Level Densities, Report BNL-NCS-51694, NewYork (1983).
- [12] SCHMIDT, K.H., DELAGRANGE, H., DUFOUR, J.P., Z. Phys., 1981, v. A308, p. 215.
- [13] IGNATYUK, A.V., STAVINSKIJ, V.S., SHUBIN, Yu.N., Nuclear Data for Reactors, Vol. 2, IAEA, Vienna (1970) 885.
- [14] KATSANOS, A.A., et al., Phys. Rev., 1970, v. C1, p. 594.
- [15] HUIZENGA, J.K., et al., Phys. Rev., 1969, v. 182, p. 1149.
- [16] KOPSCH, D., CIERJAKS, Statistical Properties of Nuclei. Plemun Press, 1972.

99-11876 (85)

Translated from Russian

UDC 539.171.016

SERIYA: JADERNYE KONSTANTY, Vypusk 1, 1999, s. 56  
(Series: Nuclear Constants, Issue No. 1 1999, p. 56)

## PHASE ANALYSIS OF THE $p^3He$ AND $pT$ ELASTIC SCATTERING CROSS-SECTIONS IN THE 0-20 MeV ENERGY REGION

L.M. Lazarev, B.M. Dzyuba

Russian Federal Nuclear Centre, All-Russia Scientific Research Institute for Experimental Physics, Sarov, Russia

### ABSTRACT

The phase shift energy dependence of proton elastic scattering by  $^3He$  and T were investigated. The Feschbach unified theory of nuclear reactions was used. Threshold phenomenon theory was developed on the basis of Feschbach theory. The phase shifts were obtained in the form of an analytical energy function taking into account 2- and multi-particle reaction thresholds as well as compound nuclear levels at  $A=4$ . The  $p+^3He$  differential elastic scattering cross-section was described theoretically in 2-11 MeV interval and in the 2-4.6 MeV interval for the  $p+T$  reaction. The theoretical parameters were obtained. Two-dimensional (with respect to the energy and scattering angles) differential cross-section tables were produced.

Elastic scattering of nuclei with  $Z<3$  by light nuclei with  $A<10$  at energies of 0-20 MeV is characterized by a set of partial waves with orbital momenta of  $l<3-4$ . The contribution of higher momenta is negligible. For this reason, series expansion of the differential cross-section to terms of spherical angular momentum functions is optimal. Representation of the energy dependence of the cross-section is a more complex matter. Usually, the scattering matrix is determined from the phase shifts [1], which means that the number of scattering parameters can be reduced to a minimum. Then the scattering parameters are calculated for those energy points where the cross-section values were measured experimentally. The two-dimensional table of scattering parameters with respect to the angular and energy variables represents the differential elastic scattering cross-section. As a rule, for intermediate scattering parameter values the cross-section is interpolated linearly or quadratically. Clearly, at some energy points such as the reaction thresholds and the compound nucleus resonances [2, 3], interpolating in this manner can lead to major errors. It therefore seems sensible to determine the dependence of the phase shifts on energy, which helps avoid interpolation errors. In addition, this also opens up the real possibility of extrapolating the elastic scattering cross-sections to regions which have not been investigated experimentally, such as the zero energy region [3]. One indisputable advantage of determining the energy dependence of the phase shifts would be a striking reduction in the number of scattering parameters (by a factor of several tens and hundreds).

To date, no work has been carried out to determine the energy dependence of the phase shifts over a wide energy interval. Refs [4, 5] studied  $p+^7\text{Li}$  elastic scattering measured in the 1.35-3 MeV incident proton energy interval [6] where two  $^7\text{Li}(p,n)^7\text{Be}$  reaction thresholds and four states of the  $^8\text{Be}$  compound nucleus are concentrated [7]. Using threshold phenomenon theory [2,3] based on Feschbach nuclear reaction theory [8], the energy dependence of the phase shifts was determined for  $l=0,1,2$ . The number of parameters is 47. They were calculated using the method of least squares from 560 experimental points. The quality of the description of the differential cross-section with the calculated parameters lay within the error limits of the experiment (1-2%). A significantly simpler energy structure of the elastic scattering cross-sections for pp, pD, DD, DT and other hydrogen pairs, and  $^4\text{He}$  was described in Ref. [9] in terms of analytical energy functions whose form is partly borrowed from Wigner's theory [10] in the vicinity of the threshold. In Ref. [9], an attempt was made to describe the experimental data using simple means and not always following strict theory. The result was satisfactory, thanks to the simplicity of the nuclear systems. In more complex systems of the  $^8\text{Be}$  type [2, 3], it is difficult to perform successful calculations without using strict theory.

Probably the first attempt at phase analysis of the  $p^3\text{He}$  elastic scattering cross-section is to be found in Refs [11, 12], using experimental data in the 1-10 MeV energy region. Here, the exchange character of the nuclear forces was studied without taking account of the energy dependence of phase shifts. Further research of this kind into  $p^3\text{He}$  elastic scattering was carried out in Refs [13, 14]. In Ref. [14], a modified approximation of the effective radius was used for the parametrization of the phase shifts and the phase mixing parameters [15], where the functions for the cotangent of the phases and the tangent of the mixing parameter are presented in the form of series in whole positive energy powers. This representation, on the whole, yields an adequate description of the experimental data in the 1-12 MeV energy interval. It was assumed that the contribution to the elastic scattering phases of the cross-sections of the  $p+^3\text{He} \rightarrow D+2p$  reaction above the 7.3 MeV threshold energy and the  $p+^3\text{He} \rightarrow n+3p$  reaction above the 10.3 MeV threshold could be disregarded up to 20 MeV owing to the small cross-sections of the reactions. The use of the phase energy dependence and mixing parameters in Ref. [14] simplified significantly the phase analysis of the 1085 experimental points and facilitated compact representation of the differential elastic scattering cross-section.

Of course, the semi-theoretical representation of the dependence of the phase shifts on energy in Refs [9, 14] is unsatisfactory owing to its lack of strictness and even arbitrary nature. A consistent theoretical approach is required which can be used to control the shape of the energy dependence of the phases and the elastic scattering cross-section, and carry out reliable calculations to the specified accuracy level. Moreover, the number of parameters required in the energy interval under investigation can be determined in advance if the singular points on the complex energy plane are known. Analytic continuation can be used to extrapolate to an uninvestigated region. Since the energy dependence is determined by orbital momentum and is not dependent on spin, the formulation of the elastic scattering cross-section in this paper will be determined only by the orbital momenta. In this case, there will be no phase shift splitting into spin multiplets. The number of parameters is reduced by a

factor of approximately three for the systems under investigation with spins of 0,1; at the same time, the accuracy of the description for the specified number of partial waves is slightly impaired. Nevertheless, the functional dependence on the energy is maintained, which will convey accurately all the details of the energy dependence of the cross-section.

## 1. Energy dependence of the phase shifts

In nuclear reaction theory, the dependence of the wave function on energy is known in the reaction threshold region.  $kR \ll 1$ ,  $\eta \gg 1$  (where  $k$  is the wave number,  $R$  is the radius of the nucleus,  $\eta$  is the Coulomb parameter) and in the vicinity of the resonance of the compound nucleus. The threshold points lie on the real axis of the energy plane, and the resonance poles are located in the lower half-plane of the non-physical sheet [16]. At the threshold points the wave function is not analytical. However, between the reaction thresholds there is no reason to assume the wave function is non-analytical [17]. Therefore, in the region between the threshold singular points we will assume that the wave function may be represented in the form of Laurent series in whole energy powers, starting from the first negative power which corresponds to the pole resonances of the compound nucleus with positive excitation energy, and going on to higher powers. The threshold properties in the two-particle channel are well known. They are second order branch points in the neutron channel or an exponential function in the channel with Coulomb repulsion. The energy dependence of the phase shift or the elastic scattering cross-section takes the form:

$$\Delta_\ell(E) = f_\ell(\eta(E))g_\ell(E, N)L_\ell(E); \quad f_\ell = \frac{2\pi\eta}{\exp(2\pi\eta)-1}; \quad g_\ell = \frac{E^{\ell+1/2+(N-2)3/2}}{[(2\ell+1)!!]^2};$$

$$L_\ell(E) = \sum_{n=0}^{n_l} b_n E^n + \sum_j A_j \operatorname{arctg} \left( \frac{\Gamma_j}{2(E - E_j)} \right); \quad \eta = Z_1 Z_2 e^2 \mu / (h^2 k), \quad \mu = \frac{m_1 m_2}{m_1 + m_2}. \quad (1)$$

where  $Z_1, Z_2$  are the charges,  $m_1, m_2$  are the masses of the interacting nuclei,  $N$  is the number of fragments in the reaction channel,  $\Gamma_j$  and  $E_j$  are the width and energy of the level of the compound nucleus. The Laurent series  $L(E)$  contains as many terms  $n_l$  for positive energy powers as is required for a satisfactory description of the cross-section. The terms with negative energy powers are arguments of the arc tangent function since, in this formula, they acquire the physical sense of a phase shift. The summation with respect to  $j$  includes all states of the compound nucleus in the energy interval under consideration. The function  $f_\ell$  characterizes the Coulomb barrier of the interacting nuclei. For the neutron channel it reverts to unity. The function  $g_\ell$  describes the threshold property in the neutron channel, including the multi-particle ( $N > 2$ ) channel, where the number of charged fragments is no greater than one.

If the number of charged fragments in the multi-particle ( $N > 2$ ) channel is greater than two, the form of the threshold property becomes more complex. As is shown in Ref. [18], in a channel comprising three charged fragments the wave function is the sum of three terms corresponding to the cyclic rearrangement of the co-ordinates of the fragments. We determine

the energy dependence at the threshold point in the following manner. We introduce a system of relative co-ordinates between the charged fragments 1 and 2 and the centre of gravity 1+2 and 3, and we assume that the 1+2 charge centre coincides with their centre of gravity. In this case, we can use the saddle point method to integrate the wave function of the system of three bodies in the vicinity of the threshold with respect to the energy of the relative movement of the subsystem 1+2. The threshold property takes the following form:

$$F_\ell(E, \xi) = f_l(\eta_{l_2}(E))f_0(\eta_{l_{+2+3}}(E\xi)); \quad 0 \leq \xi \leq 1. \quad (2)$$

The saddle point  $\xi$  may be estimated with a high level of accuracy as the integrand is fairly sharply peaked.

The threshold property (2) with no cyclic rearrangement of the co-ordinates will be assumed to be adequate to describe the energy dependence of the phases in the channel with three charged fragments.

Above the reaction threshold, the scattering phase must be a complex value to fit with the relation of unitarity [1] imposed on the scattering matrix. The imaginary part of the phase is positive so as to ensure that the absolute value of the elastic scattering matrix element remains less than unity. It reflects the contribution of the reaction cross-sections to the elastic scattering cross-section. The phase shift in the 0-20 MeV energy interval may be represented as a function which takes the following form:

$$\delta_l(E) = \Delta_l(E) + \sum_{m=1}^M D_{lm}(E_m) \Theta(E_m), \quad E_m = E - E_{qm}, \quad \Theta(E_m) = \begin{cases} 1, & E > E_m \\ 0, & E < E_m \end{cases}, \quad (3)$$

where the real part is described using the formulae in expression (1) with N=2. The virtual part contains the sum of the phases over the reaction channels. M is the number of reaction channels. For proton scattering by  ${}^3\text{He}$ , the D+2p channel phase is included above the  $E_{q1}=7.3$  MeV threshold (5.494 MeV CM) and is described by the function:

$$\begin{aligned} D_{l1}(E_1) &= F_1(E_1, \xi) g_1(E_1, N=3) L_1(E_1), \quad E_1 = E - E_{q1}; \\ F_1(E_1) &= f_1(\eta_{pp}(E_1)) f_0(\eta_{2,p,d}(\xi_1 E_1)). \end{aligned} \quad (4)$$

The n+3p channel phase makes a contribution above the  $E_{q2}=10.3$  MeV threshold (7.718 MeV CM) and is characterized by the function:

$$\begin{aligned} D_{l2}(E_2) &= F_1(E_2, \xi_2) g_1(E_2, N=4) L_1(E_2), \quad E_2 = E - E_{q2}; \\ F_1(E_2) &= f_1(\eta_{pp}(E_2)) f_0(\eta_{2,p,p}(\xi_2 E_2)). \end{aligned} \quad (5)$$

The Laurent series in phases (3)-(5) each contain four terms which correspond to the formation of the resonance states of the  ${}^4\text{Li}$  compound nucleus; these are taken from the cross-section and spin correlation data in Ref. [14] and the elastic scattering data in Ref. [19]. In

these series, the parameters  $b$  and  $A_j$  differ, and the parameters  $E_j$  and  $\Gamma_j$  for each state are the same in all phases. Although the reaction thresholds are higher than some compound nucleus levels, all the levels can be left in the reaction phases thanks to the cut-off factor  $\Theta(E)$ .

In the nuclear system pT at  $E_p > 0$ , there are four thresholds for the  $n+^3\text{He}$ ,  $d+d$ ,  $d+p+n$ ,  $2p+2n$  reaction channels ( $M=4$ ) and ten levels of the  ${}^4\text{He}$  compound nucleus [19]. The phase shift is represented as a function taking the form of expression (3) with an imaginary part comprising four phases  $D_{lm}$  according to the number of open reaction channels in the 0-20 MeV energy region. Above the threshold of the  $n+^3\text{He}$  channel ( $E_{q1}=0.763$  CM), the phase  $D_{l1}$  is described using formula (1) with the function  $f_l=1$ . Above the second threshold of the  $d+d$  channel ( $E_{q2}=4.033$  MeV), the phase  $D_{l2}$  is given by formula (1). After the third threshold of the  $d+p+n$  channel ( $E_{q3}=6.257$  MeV), the phase is represented by function (1) with  $N=3$ ; and, after the fourth threshold of the  $2p+2n$  channel ( $E_{q4}=8.482$  MeV), by function (1) with  $N=4$ . The  $p+T$  elastic scattering phase shift (real part) is given by function (1) where  $N=2$ . The Laurent series  $L_l(E)$  for all phases include ten resonance terms which correspond to the excited levels of the compound nucleus. The parameters  $E_j$  and  $\Gamma_j$  are the same for each level, and the parameters  $b$  and  $A_j$  are different.

## 2. Elastic scattering cross-section

The differential elastic scattering cross-section in our calculations is represented by the following energy function [1]:

$$d\sigma/d\Omega = g|A(\theta, E)|^2; \quad A(\theta, E) = f_c(\theta, E) + f_N(\theta, E) \quad (6)$$

where the Coulomb and nuclear scattering amplitudes take the standard form:

$$\begin{aligned} f_c(\theta, E) &= -\eta \exp(-2i\eta \ln(\sin(\theta/2))) / (2k(\sin(\theta/2))^2) \\ f_1(\theta, E) &= \frac{1}{2ik} \sum_l (2l+1) e^{2i\omega_l} (e^{2i\delta_l} - 1) P_l(\cos\theta), \\ \omega_l &= \sum_{s=1}^l \operatorname{arctg}(\eta/s), \quad \omega_0 = 0. \end{aligned} \quad (7)$$

Here,  $g$  is the statistical multiplier,  $\theta$  is the scattering angle in the direction of the solid angle  $\Omega$ ,  $\omega_l$  is the Coulomb scattering phase,  $P_l$  is the Legendre polynomial. The dependence of the phase shift on energy is determined using formulae (1)-(5). The parameters in the phases were varied using the method of least squares with a view to achieving an optimal description of the experimental data for the elastic scattering cross-section. The data with polarized particles were not used in the calculations.

## 3. Phase analysis of the $p+{}^3\text{He}$ elastic scattering cross-section

A preliminary phase analysis was carried out using the traditional method: at each energy point from the experimental data the phase shifts were determined for orbital momenta

of  $l=0,1,2$ . The theoretical shape of the cross-section was taken from Ref. [13] where the cross-section is represented as the sum of eight terms consisting in the squares of the absolute amplitude values which describe the eight independent terms in the total amplitude to account for all possible spin correlations. Taking into account spin multiplets, the number of phase shifts is 11 plus one mixing parameter. If we disregard spin dependence, the number of phase shifts is three and one mixing parameter. At energies of  $E_p=1; 4$  MeV, in both cases the description of the angular distributions differs significantly (see Figs 1, 2). The quality of the description of the angular distributions improves substantially when the mixing parameter is introduced into the calculations both for the 11 phases and the 3 phases. The accuracy of the description changes on average from 15% to 5%.

Subsequently, calculations were carried out using formulae (6)-(7) with the energy-dependent phase shifts (1)-(5). Figs 3 and 4 show the results of the calculation of the angular distributions of protons elastically scattered by  $^3\text{He}$  nuclei at the same energies ( $E_p=1; 4$  MeV) as Figs 1 and 2, for the purpose of comparison with the calculations performed using the method from Ref. [13]. Comparing Figs 1 and 2 with Figs 3 and 4, it can be seen that introducing the theoretical dependence on energy into the phase shifts improves the description of the elastic scattering cross-section. The phase shift parameters in Table I were determined using a two-dimensional experimental data array comprising 241 points (see Table II) taken from the excitation and angular distribution functions of Refs [20-22]. The number of partial waves was assumed to be three:  $l=0,1,2$ . From Table II it is clear that the accuracy level of the description amounts to a few per cent, and only isolated points yield a divergence of the order of 20%. The parameters of the levels of the compound nucleus are not included since the description of the differential cross-section did not require their use. For this reason, the coefficients  $b$  continue to figure in the Laurent series  $L_l(E)$  at positive energy powers. In the energy region below the first threshold ( $E_p$  CM  $<5.494$  MeV), the number of parameters is 6: three coefficients  $b$  to determine the  $\delta_0$  phase at the zero, first and second energy powers; two coefficients  $b$  at the zero and first energy powers to determine the  $\delta_1$  phase; and one coefficient  $b$  at the zero energy power to determine  $\delta_2$ . This procedure for setting the coefficients  $b$  was adopted to even out the energy powers when determining the energy dependence of phase shifts with different orbital momenta. Five parameters  $b$  were set in the first open reaction channel. In addition, in each open multi-particle channel one parameter  $\xi$  comes into play when three charged fragments are formed in the channel. These may be determined using the saddle point method by integration, or using the method of least squares by varying the parameters. We varied the parameters  $\xi$  during the initial fitting stage, and they were then fixed at the values given in Table I to speed up the variation process.

#### 4. Phase analysis of the pT elastic scattering cross-section

The dependence of the phase shifts on channel spin was ignored in the analysis. The calculations were carried out using formulae (6)-(7) taking into account the orbital momenta  $l=0-4$ . The theoretical dependence of the phase shifts on energy in expressions (1)-(5) was used. The presence of four reaction thresholds ( $M=4$  in expression (3)) and ten levels of the compound nucleus significantly increases the number of parameters. In order to simplify the calculations, the influence of the levels of the  $^4\text{He}$  compound nucleus were ignored:  $A_j=0$  in the  $L_l(E)$  function. The coefficients  $b_l$  are non-zero for the lowest energy powers:  $n=0$  for all values of  $l,m$  and  $n=1$  for  $l=0,1$ , and  $n=2$  for  $l=0$ . In total, there are

8 parameters in each channel irrespective of the number of fragments in the channel since the number of charged fragments in the channel does not exceed two, i.e. the parameter  $\xi$  does not come into play. In the  $E_p=2.12\text{-}4.6$  MeV energy region [23-24] two channels are open and, using 16 parameters (see Table III), an accuracy level of a few percent is achieved in the description of the differential cross-section, as may be seen from Table IV.

## Conclusion

The phase analysis of the  $p^3He$  and  $pT$  elastic scattering cross-sections using the theoretical dependence of the phase shifts on energy demonstrated the advantages of this approach over traditional point-by-point phase analysis. These include not only the higher quality description, as can be seen by comparing Figs 1-4, but also the more compact representation of the differential cross-section. In the traditional description the cross-section is presented in the form of a two-dimensional table with respect to the angular and energy variables. Apart from the analogous representation in our method, the elastic scattering phase shifts and cross-section can be notated in analytical form by adding a table of parameter values. The number of parameters amounts to a few tens, whereas the tabular representation of the cross-section contains thousands of numbers. In traditional phase analysis it is impossible to be sure that interpolations are correct, since no theoretical dependence of the cross-section on energy is available. Our method permits confident interpolation, and even extrapolation to the zero energy region. Extrapolation to the high energy region would require further research, but our calculations with the parameter values obtained showed that extrapolation 1-2 MeV higher is possible with the same accuracy. The fact that, though we ignored the dependence of the phase shifts on spin, this did not prevent us from obtaining a highly accurate description of the cross-section, indicates that the dependence of the cross-section on spin is low. Where the effect of spin cannot be ignored, such as when describing the scattering of polarized particles, , the dependence of the phase shifts on energy remains the same. The dependence of the mixing parameter on energy was not studied. It should be noted that, though the description of  $p+^3He$  elastic scattering in the 0.3-11 MeV energy region yielded good results without including the pole terms characterizing the levels of the compound nucleus in formulae (1)-(5), the description of  $p+T$  scattering in the 0.3-2 MeV energy region [25] showed irregularities in the behaviour of the parameters. This indicates that the pole terms should be included in the calculation formulae. In the 2.12-4.6 MeV energy region, where there are no levels of the  ${}^4He$  compound nucleus, the parameters are constants which accurately describe the experimental data without including the pole terms in the calculation formulae (see Tables III, IV).

Fig. 5 shows the energy dependence of the  $p+^3He$  scattering phase shifts in the energy interval below the first reaction threshold. Comparing this with the calculations in Ref. [13], we can see that the phase shift values do not coincide for the same orbital momenta. Moreover, the signs are the same only for the  $\delta_0$  phase. Clearly, our set of phases is to be preferred because of the improved description of the experimental data in the representation of the elastic scattering cross-section using formulae (6-7).

TABLE I. PARAMETERS OF THE ENERGY DEPENDENCE OF THE  $p+^3\text{He}$  ELASTIC SCATTERING PHASE SHIFTS  
( $L_i(E)$  PARAMETERS IN TWO ENERGY REGIONS)

1	Parameter	$E_p < E_{q1}$	$E_{q1} < E_p < E_{q2}$
0	$b_{00}$ ,	-0.13908E+01	0.54759E+00
0	$b_{01}$ , MeV $^{-1}$	0.31242E+00	0.0
0	$b_{02}$ , MeV $^{-2}$	-0.50985E-01	0.0
1	$b_{10}$	0.24412E+01	0.13569E+01
1	$b_{11}$ , MeV $^{-1}$	-0.32712E+00	-0.37075E+00
2	$b_{20}$	-0.80615E+00	-0.43779E+00
2	$b_{21}$ , MeV $^{-1}$	0.0	0.39203E+00
	$\xi_1$	0.0	0.23400E+00

Proton energy given in MeV (LAB)

TABLE II. THEORETICAL DESCRIPTION OF THE  $p+^3\text{He}$  DIFFERENTIAL ELASTIC SCATTERING CROSS-SECTION  $\sigma$  ( $\theta, E_p$ ) RELATIVE TO THE ANGLE  $\theta$  (CM) AND THE ENERGY  $E_p$  (LAB)

No.	$\theta$ , degrees	$E_p$ , MeV	$\sigma_{\text{theor}}$	$\sigma_{\text{exp}}$	$(\sigma_{\text{theor}} - \sigma_{\text{exp}}) / \sigma_{\text{exp}} \%$
1	0.17060E+03	0.29100E+01	0.28217E+00	0.27170E+00	-0.38523E+01
2	0.17060E+03	0.30412E+01	0.28365E+00	0.26510E+00	-0.69965E+01
3	0.17060E+03	0.31898E+01	0.28388E+00	0.26290E+00	-0.79797E+01
4	0.17060E+03	0.33818E+01	0.28190E+00	0.25630E+00	-0.99875E+01
5	0.17060E+03	0.35122E+01	0.27911E+00	0.24300E+00	-0.14859E+02
6	0.17060E+03	0.36803E+01	0.27385E+00	0.24530E+00	-0.11641E+02
7	0.17060E+03	0.38108E+01	0.26856E+00	0.23200E+00	-0.15757E+02
8	0.17060E+03	0.40695E+01	0.25523E+00	0.21540E+00	-0.18493E+02
9	0.17060E+03	0.44093E+01	0.23326E+00	0.20890E+00	-0.11660E+02
10	0.17060E+03	0.45368E+01	0.22415E+00	0.20670E+00	-0.84408E+01
11	0.17060E+03	0.47063E+01	0.21171E+00	0.20450E+00	-0.35247E+01
12	0.17060E+03	0.49853E+01	0.19148E+00	0.18790E+00	-0.19077E+01
13	0.17060E+03	0.51330E+01	0.18151E+00	0.18800E+00	0.34510E+01
14	0.17060E+03	0.53048E+01	0.17114E+00	0.17910E+00	0.44466E+01
15	0.17060E+03	0.54315E+01	0.16462E+00	0.17920E+00	0.81344E+01
16	0.17060E+03	0.56025E+01	0.15781E+00	0.17140E+00	0.79314E+01
17	0.17060E+03	0.57937E+01	0.15329E+00	0.16820E+00	0.88638E+01
18	0.17060E+03	0.59220E+01	0.15188E+00	0.16150E+00	0.59584E+01
19	0.17060E+03	0.60705E+01	0.15113E+00	0.15930E+00	0.51302E+01
20	0.17060E+03	0.61995E+01	0.15057E+00	0.15270E+00	0.13963E+01
21	0.17060E+03	0.63697E+01	0.14890E+00	0.14830E+00	-0.40342E+00
22	0.17060E+03	0.64980E+01	0.14611E+00	0.14280E+00	-0.23199E+01
23	0.17060E+03	0.66683E+01	0.13873E+00	0.13950E+00	0.55051E+00
24	0.17060E+03	0.68370E+01	0.12504E+00	0.13510E+00	0.74480E+01
25	0.17060E+03	0.80775E+01	0.78494E-01	0.11300E+00	0.30536E+02
26	0.15500E+03	0.75000E+00	0.12751E+00	0.11800E+00	-0.80613E+01

27	0.15500E+03	0.82500E+00	0.13349E+00	0.12500E+00	-0.67947E+01
28	0.15500E+03	0.90000E+00	0.13970E+00	0.13200E+00	-0.58355E+01
29	0.15500E+03	0.97500E+00	0.14600E+00	0.14100E+00	-0.35486E+01
30	0.15500E+03	0.10500E+01	0.15230E+00	0.15000E+00	-0.15357E+01
31	0.15500E+03	0.11250E+01	0.15854E+00	0.15700E+00	-0.98069E+00
32	0.15500E+03	0.12000E+01	0.16467E+00	0.16400E+00	-0.40702E+00
33	0.15500E+03	0.12750E+01	0.17066E+00	0.16800E+00	-0.15804E+01
34	0.15500E+03	0.13500E+01	0.17648E+00	0.17300E+00	-0.20110E+01
35	0.15500E+03	0.14250E+01	0.18212E+00	0.17800E+00	-0.23153E+01
36	0.15500E+03	0.15000E+01	0.18757E+00	0.18200E+00	-0.30593E+01
37	0.15500E+03	0.15750E+01	0.19281E+00	0.18600E+00	-0.36599E+01
38	0.15500E+03	0.16500E+01	0.19783E+00	0.19100E+00	-0.35758E+01
39	0.15500E+03	0.17250E+01	0.20263E+00	0.19800E+00	-0.23365E+01
40	0.15500E+03	0.18000E+01	0.20719E+00	0.20500E+00	-0.10674E+01
41	0.15500E+03	0.18750E+01	0.21151E+00	0.21000E+00	-0.71791E+00
42	0.15500E+03	0.19500E+01	0.21558E+00	0.21400E+00	-0.73667E+00
43	0.15500E+03	0.20250E+01	0.21939E+00	0.21800E+00	-0.63612E+00
44	0.15500E+03	0.21000E+01	0.22293E+00	0.22300E+00	0.31249E-01
45	0.15500E+03	0.21750E+01	0.22620E+00	0.22600E+00	-0.88122E-01
46	0.15500E+03	0.22500E+01	0.22919E+00	0.23000E+00	0.35426E+00
47	0.15500E+03	0.23250E+01	0.23188E+00	0.23100E+00	-0.38118E+00
48	0.15500E+03	0.24000E+01	0.23428E+00	0.23200E+00	-0.98161E+00
49	0.15500E+03	0.24750E+01	0.23637E+00	0.23300E+00	-0.14456E+01
50	0.15500E+03	0.25500E+01	0.23815E+00	0.23410E+00	-0.17283E+01
51	0.15500E+03	0.26250E+01	0.23960E+00	0.23430E+00	-0.22638E+01
52	0.15500E+03	0.27000E+01	0.24074E+00	0.23420E+00	-0.27910E+01
53	0.15500E+03	0.27750E+01	0.24154E+00	0.23410E+00	-0.31774E+01
54	0.15500E+03	0.28500E+01	0.24200E+00	0.23400E+00	-0.34208E+01
55	0.15500E+03	0.29250E+01	0.24213E+00	0.23200E+00	-0.43675E+01
56	0.15500E+03	0.30000E+01	0.24192E+00	0.23000E+00	-0.51822E+01
57	0.15500E+03	0.30750E+01	0.24136E+00	0.23100E+00	-0.44862E+01
58	0.15500E+03	0.31500E+01	0.24046E+00	0.23200E+00	-0.36485E+01
59	0.15500E+03	0.32250E+01	0.23922E+00	0.22930E+00	-0.43282E+01
60	0.15500E+03	0.33000E+01	0.23765E+00	0.22730E+00	-0.45515E+01
61	0.15500E+03	0.33750E+01	0.23573E+00	0.22530E+00	-0.46300E+01
62	0.15500E+03	0.34500E+01	0.23349E+00	0.22300E+00	-0.47029E+01
63	0.15500E+03	0.35250E+01	0.23092E+00	0.22300E+00	-0.35519E+01
64	0.15500E+03	0.37500E+01	0.22137E+00	0.21400E+00	-0.34459E+01
65	0.15500E+03	0.45000E+01	0.17416E+00	0.18600E+00	0.63649E+01
66	0.15500E+03	0.52500E+01	0.12218E+00	0.15900E+00	0.23159E+02
67	0.15500E+03	0.60000E+01	0.97970E-01	0.12200E+00	0.19697E+02
68	0.88254E+02	0.22500E+00	0.51819E+00	0.52480E+00	0.12604E+01
69	0.99164E+02	0.22500E+00	0.38034E+00	0.38340E+00	0.79760E+00
70	0.10947E+03	0.22500E+00	0.30024E+00	0.30710E+00	0.22339E+01
71	0.11916E+03	0.22500E+00	0.25048E+00	0.25300E+00	0.99675E+00
72	0.12825E+03	0.22500E+00	0.21804E+00	0.22290E+00	0.21819E+01
73	0.88254E+02	0.30000E+00	0.33858E+00	0.34200E+00	0.99961E+00
74	0.99164E+02	0.30000E+00	0.25753E+00	0.26040E+00	0.11023E+01
75	0.10947E+03	0.30000E+00	0.20989E+00	0.21240E+00	0.11811E+01

76	0.11916E+03	0.30000E+00	0.18001E+00	0.18490E+00	0.26421E+01
77	0.12825E+03	0.30000E+00	0.16039E+00	0.16530E+00	0.29702E+01
78	0.13678E+03	0.30000E+00	0.14709E+00	0.15050E+00	0.22686E+01
79	0.14479E+03	0.30000E+00	0.13792E+00	0.14160E+00	0.26022E+01
80	0.76779E+02	0.37500E+00	0.35494E+00	0.35630E+00	0.38194E+00
81	0.88254E+02	0.37500E+00	0.25559E+00	0.25820E+00	0.10120E+01
82	0.99164E+02	0.37500E+00	0.20180E+00	0.20300E+00	0.59208E+00
83	0.10947E+03	0.37500E+00	0.17000E+00	0.17180E+00	0.10505E+01
84	0.11916E+03	0.37500E+00	0.14999E+00	0.15270E+00	0.17738E+01
85	0.12825E+03	0.37500E+00	0.13685E+00	0.13940E+00	0.18301E+01
86	0.13678E+03	0.37500E+00	0.12795E+00	0.12990E+00	0.14977E+01
87	0.14479E+03	0.37500E+00	0.12184E+00	0.12470E+00	0.22917E+01
88	0.15237E+03	0.37500E+00	0.11762E+00	0.12090E+00	0.27171E+01
89	0.15959E+03	0.37500E+00	0.11474E+00	0.11810E+00	0.28451E+01
90	0.16655E+03	0.37500E+00	0.11288E+00	0.11620E+00	0.28584E+01
91	0.76779E+02	0.45000E+00	0.28022E+00	0.28000E+00	-0.80319E-01
92	0.88254E+02	0.45000E+00	0.21007E+00	0.21110E+00	0.48957E+00
93	0.99164E+02	0.45000E+00	0.17201E+00	0.17120E+00	-0.47474E+00
94	0.10947E+03	0.45000E+00	0.14958E+00	0.15010E+00	0.34370E+00
95	0.11916E+03	0.45000E+00	0.13559E+00	0.13660E+00	0.73741E+00
96	0.12825E+03	0.45000E+00	0.12651E+00	0.12720E+00	0.53869E+00
97	0.13678E+03	0.45000E+00	0.12046E+00	0.12190E+00	0.11773E+01
98	0.14479E+03	0.45000E+00	0.11638E+00	0.11760E+00	0.10414E+01
99	0.15237E+03	0.45000E+00	0.11359E+00	0.11590E+00	0.19913E+01
100	0.15959E+03	0.45000E+00	0.11173E+00	0.11380E+00	0.18225E+01
101	0.16655E+03	0.45000E+00	0.11053E+00	0.11270E+00	0.19239E+01
102	0.17332E+03	0.45000E+00	0.10987E+00	0.11130E+00	0.12872E+01
103	0.76779E+02	0.52500E+00	0.23365E+00	0.23280E+00	-0.36465E+00
104	0.88254E+02	0.52500E+00	0.18205E+00	0.18160E+00	-0.25022E+00
105	0.99164E+02	0.52500E+00	0.15428E+00	0.15360E+00	-0.44583E+00
106	0.10947E+03	0.52500E+00	0.13819E+00	0.13800E+00	-0.13898E+00
107	0.11916E+03	0.52500E+00	0.12842E+00	0.12880E+00	0.29688E+00
108	0.12825E+03	0.52500E+00	0.12230E+00	0.12260E+00	0.24530E+00
109	0.13678E+03	0.52500E+00	0.11839E+00	0.11890E+00	0.42604E+00
110	0.14479E+03	0.52500E+00	0.11588E+00	0.11660E+00	0.62164E+00
111	0.15237E+03	0.52500E+00	0.11424E+00	0.11520E+00	0.83191E+00
112	0.15959E+03	0.52500E+00	0.11319E+00	0.11410E+00	0.79365E+00
113	0.16655E+03	0.52500E+00	0.11255E+00	0.11390E+00	0.11860E+01
114	0.17332E+03	0.52500E+00	0.11220E+00	0.11320E+00	0.88353E+00
115	0.76779E+02	0.60000E+00	0.20207E+00	0.19940E+00	-0.13404E+01
116	0.88254E+02	0.60000E+00	0.16330E+00	0.16180E+00	-0.92702E+00
117	0.99164E+02	0.60000E+00	0.14287E+00	0.14130E+00	-0.11089E+01
118	0.10947E+03	0.60000E+00	0.13148E+00	0.13030E+00	-0.90249E+00
119	0.11916E+03	0.60000E+00	0.12497E+00	0.12490E+00	-0.54518E-01
120	0.12825E+03	0.60000E+00	0.12124E+00	0.12060E+00	-0.52947E+00
121	0.13678E+03	0.60000E+00	0.11913E+00	0.11930E+00	0.14432E+00
122	0.14479E+03	0.60000E+00	0.11797E+00	0.11810E+00	0.11371E+00
123	0.15237E+03	0.60000E+00	0.11735E+00	0.11770E+00	0.29860E+00
124	0.15959E+03	0.60000E+00	0.11704E+00	0.11760E+00	0.47748E+00

125	0.16655E+03	0.60000E+00	0.11689E+00	0.11820E+00	0.11051E+01
126	0.17332E+03	0.60000E+00	0.11683E+00	0.11790E+00	0.90406E+00
127	0.76779E+02	0.67500E+00	0.17927E+00	0.17450E+00	-0.27340E+01
128	0.88254E+02	0.67500E+00	0.14989E+00	0.14690E+00	-0.20373E+01
129	0.99164E+02	0.67500E+00	0.13503E+00	0.13180E+00	-0.24510E+01
130	0.10947E+03	0.67500E+00	0.12737E+00	0.12520E+00	-0.17311E+01
131	0.11916E+03	0.67500E+00	0.12357E+00	0.12140E+00	-0.17864E+01
132	0.12825E+03	0.67500E+00	0.12190E+00	0.12030E+00	-0.13340E+01
133	0.13678E+03	0.67500E+00	0.12140E+00	0.12020E+00	-0.10001E+01
134	0.14479E+03	0.67500E+00	0.12149E+00	0.12080E+00	-0.57068E+00
135	0.15237E+03	0.67500E+00	0.12183E+00	0.12140E+00	-0.35324E+00
136	0.15959E+03	0.67500E+00	0.12222E+00	0.12200E+00	-0.18325E+00
137	0.16655E+03	0.67500E+00	0.12256E+00	0.12260E+00	0.30441E-01
138	0.17332E+03	0.67500E+00	0.12279E+00	0.12330E+00	0.41767E+00
139	0.76779E+02	0.75000E+00	0.16199E+00	0.15770E+00	-0.27172E+01
140	0.88254E+02	0.75000E+00	0.13979E+00	0.13650E+00	-0.24087E+01
141	0.99164E+02	0.75000E+00	0.12935E+00	0.12530E+00	-0.32290E+01
142	0.10947E+03	0.75000E+00	0.12478E+00	0.12160E+00	-0.26133E+01
143	0.11916E+03	0.75000E+00	0.12333E+00	0.12140E+00	-0.15923E+01
144	0.12825E+03	0.75000E+00	0.12354E+00	0.12170E+00	-0.15098E+01
145	0.13678E+03	0.75000E+00	0.12454E+00	0.12260E+00	-0.15799E+01
146	0.14479E+03	0.75000E+00	0.12582E+00	0.12440E+00	-0.11421E+01
147	0.15237E+03	0.75000E+00	0.12709E+00	0.12590E+00	-0.94801E+00
148	0.15959E+03	0.75000E+00	0.12819E+00	0.12780E+00	-0.30131E+00
149	0.16655E+03	0.75000E+00	0.12901E+00	0.12820E+00	-0.62946E+00
150	0.17332E+03	0.75000E+00	0.12951E+00	0.12960E+00	0.67745E-01
151	0.67830E+02	0.17850E+01	0.84524E-01	0.83000E-01	-0.18364E+01
152	0.73830E+02	0.17850E+01	0.83552E-01	0.87000E-01	0.39637E+01
153	0.79700E+02	0.17850E+01	0.84011E-01	0.85000E-01	0.11640E+01
154	0.85440E+02	0.17850E+01	0.85948E-01	0.85000E-01	-0.11155E+01
155	0.91040E+02	0.17850E+01	0.89380E-01	0.88000E-01	-0.15682E+01
156	0.96490E+02	0.17850E+01	0.94255E-01	0.95000E-01	0.78379E+00
157	0.10180E+03	0.17850E+01	0.10048E+00	0.10100E+00	0.51714E+00
158	0.10690E+03	0.17850E+01	0.10778E+00	0.10500E+00	-0.26498E+01
159	0.11190E+03	0.17850E+01	0.11612E+00	0.11200E+00	-0.36782E+01
160	0.11680E+03	0.17850E+01	0.12529E+00	0.12200E+00	-0.26977E+01
161	0.12150E+03	0.17850E+01	0.13486E+00	0.13800E+00	0.22722E+01
162	0.12600E+03	0.17850E+01	0.14457E+00	0.15000E+00	0.36176E+01
163	0.13040E+03	0.17850E+01	0.15440E+00	0.17400E+00	0.11262E+02
164	0.13470E+03	0.17850E+01	0.16415E+00	0.19300E+00	0.14947E+02
165	0.67830E+02	0.19575E+01	0.82623E-01	0.90000E-01	0.81972E+01
166	0.73830E+02	0.19575E+01	0.80999E-01	0.91000E-01	0.10991E+02
167	0.79700E+02	0.19575E+01	0.80775E-01	0.83000E-01	0.26805E+01
168	0.85440E+02	0.19575E+01	0.82147E-01	0.81000E-01	-0.14163E+01
169	0.91040E+02	0.19575E+01	0.85221E-01	0.82000E-01	-0.39284E+01
170	0.96490E+02	0.19575E+01	0.89997E-01	0.89000E-01	-0.11201E+01
171	0.10180E+03	0.19575E+01	0.96397E-01	0.94000E-01	-0.25505E+01
172	0.10690E+03	0.19575E+01	0.10415E+00	0.10400E+00	-0.14311E+00
173	0.11190E+03	0.19575E+01	0.11319E+00	0.11500E+00	0.15737E+01

174	0.11680E+03	0.19575E+01	0.12330E+00	0.12800E+00	0.36730E+01
175	0.12150E+03	0.19575E+01	0.13398E+00	0.14100E+00	0.49784E+01
176	0.12600E+03	0.19575E+01	0.14492E+00	0.15200E+00	0.46585E+01
177	0.13040E+03	0.19575E+01	0.15608E+00	0.15200E+00	-0.26845E+01
178	0.13470E+03	0.19575E+01	0.16722E+00	0.18600E+00	0.10097E+02
179	0.67830E+02	0.21675E+01	0.83080E-01	0.10600E+00	0.21622E+02
180	0.73830E+02	0.21675E+01	0.80000E-01	0.94000E-01	0.14893E+02
181	0.79700E+02	0.21675E+01	0.78376E-01	0.91000E-01	0.13873E+02
182	0.85440E+02	0.21675E+01	0.78552E-01	0.86000E-01	0.86610E+01
183	0.91040E+02	0.21675E+01	0.80733E-01	0.88000E-01	0.82583E+01
184	0.96490E+02	0.21675E+01	0.84974E-01	0.91000E-01	0.66215E+01
185	0.10180E+03	0.21675E+01	0.91222E-01	0.97000E-01	0.59567E+01
186	0.10690E+03	0.21675E+01	0.99194E-01	0.10700E+00	0.72956E+01
187	0.11190E+03	0.21675E+01	0.10881E+00	0.11300E+00	0.37097E+01
188	0.11680E+03	0.21675E+01	0.11981E+00	0.12400E+00	0.33777E+01
189	0.12150E+03	0.21675E+01	0.13164E+00	0.13400E+00	0.17601E+01
190	0.12600E+03	0.21675E+01	0.14391E+00	0.14700E+00	0.20995E+01
191	0.13040E+03	0.21675E+01	0.15656E+00	0.14700E+00	-0.65064E+01
192	0.13470E+03	0.21675E+01	0.16929E+00	0.15300E+00	-0.10649E+02
193	0.13880E+03	0.21675E+01	0.18152E+00	0.16200E+00	-0.12050E+02
194	0.67830E+02	0.24150E+01	0.86654E-01	0.12000E+00	0.27788E+02
195	0.73830E+02	0.24150E+01	0.81203E-01	0.10500E+00	0.22664E+02
196	0.79700E+02	0.24150E+01	0.77339E-01	0.96000E-01	0.19439E+02
197	0.85440E+02	0.24150E+01	0.75556E-01	0.93000E-01	0.18757E+02
198	0.91040E+02	0.24150E+01	0.76164E-01	0.92000E-01	0.17213E+02
199	0.96490E+02	0.24150E+01	0.79284E-01	0.92000E-01	0.13821E+02
200	0.10180E+03	0.24150E+01	0.84889E-01	0.94000E-01	0.96922E+01
201	0.10690E+03	0.24150E+01	0.92698E-01	0.10100E+00	0.82195E+01
202	0.11190E+03	0.24150E+01	0.10260E+00	0.10900E+00	0.58719E+01
203	0.11680E+03	0.24150E+01	0.11431E+00	0.12200E+00	0.63043E+01
204	0.12150E+03	0.24150E+01	0.12719E+00	0.13100E+00	0.29097E+01
205	0.12600E+03	0.24150E+01	0.14077E+00	0.14500E+00	0.29138E+01
206	0.13040E+03	0.24150E+01	0.15496E+00	0.15400E+00	-0.62409E+00
207	0.13470E+03	0.24150E+01	0.16938E+00	0.16700E+00	-0.14261E+01
208	0.13880E+03	0.24150E+01	0.18335E+00	0.18800E+00	0.24754E+01
209	0.14280E+03	0.24150E+01	0.19689E+00	0.20100E+00	0.20472E+01
210	0.18630E+02	0.30000E+01	0.44368E+00	0.47800E+00	0.71797E+01
211	0.22600E+02	0.30000E+01	0.22731E+00	0.24900E+00	0.87100E+01
212	0.26570E+02	0.30000E+01	0.16832E+00	0.18730E+00	0.10132E+02
213	0.30500E+02	0.30000E+01	0.15332E+00	0.17660E+00	0.13180E+02
214	0.34420E+02	0.30000E+01	0.15019E+00	0.17280E+00	0.13083E+02
215	0.38230E+02	0.30000E+01	0.14924E+00	0.16890E+00	0.11638E+02
216	0.42200E+02	0.30000E+01	0.14739E+00	0.16400E+00	0.10128E+02
217	0.58920E+02	0.30000E+01	0.12253E+00	0.13000E+00	0.57469E+01
218	0.77020E+02	0.30000E+01	0.85091E-01	0.90300E-01	0.57683E+01
219	0.94030E+02	0.30000E+01	0.67083E-01	0.71300E-01	0.59147E+01
220	0.10970E+03	0.30000E+01	0.79942E-01	0.84600E-01	0.55063E+01
221	0.12400E+03	0.30000E+01	0.11840E+00	0.12220E+00	0.31121E+01
222	0.13280E+03	0.30000E+01	0.15168E+00	0.15160E+00	-0.54060E-01

223	0.14500E+03	0.30000E+01	0.20275E+00	0.19480E+00	-0.40806E+01
224	0.15620E+03	0.30000E+01	0.24613E+00	0.23850E+00	-0.31994E+01
225	0.17060E+03	0.30000E+01	0.28331E+00	0.27040E+00	-0.47746E+01
226	0.18630E+02	0.41325E+01	0.29027E+00	0.31100E+00	0.66649E+01
227	0.22600E+02	0.41325E+01	0.22478E+00	0.25200E+00	0.10802E+02
228	0.26570E+02	0.41325E+01	0.21769E+00	0.24200E+00	0.10044E+02
229	0.30500E+02	0.41325E+01	0.22133E+00	0.24300E+00	0.89185E+01
230	0.34420E+02	0.41325E+01	0.22426E+00	0.23600E+00	0.49729E+01
231	0.38230E+02	0.41325E+01	0.22403E+00	0.23100E+00	0.30173E+01
232	0.42200E+02	0.41325E+01	0.22032E+00	0.22500E+00	0.20778E+01
233	0.58920E+02	0.41325E+01	0.17648E+00	0.16270E+00	-0.84691E+01
234	0.77020E+02	0.41325E+01	0.10757E+00	0.95100E-01	-0.13112E+02
235	0.94030E+02	0.41325E+01	0.55068E-01	0.55900E-01	0.14888E+01
236	0.10970E+03	0.41325E+01	0.40704E-01	0.54800E-01	0.25722E+02
237	0.12400E+03	0.41325E+01	0.65504E-01	0.83600E-01	0.21646E+02
238	0.13280E+03	0.41325E+01	0.97061E-01	0.11040E+00	0.12083E+02
239	0.14500E+03	0.41325E+01	0.15294E+00	0.15670E+00	0.23990E+01
240	0.15620E+03	0.41325E+01	0.20479E+00	0.19610E+00	-0.44295E+01
241	0.17060E+03	0.41325E+01	0.25149E+00	0.23390E+00	-0.75205E+01

Note:  $\sigma_{\text{theor}}$  is the theoretical cross-section value,  $\sigma_{\text{exp}}$  is the experimental cross-section value; the cross-sections are given in barns per steradian.

TABLE III. PARAMETERS OF THE ENERGY DEPENDENCE OF THE pT ELASTIC SCATTERING PHASE SHIFTS

1	Parameter	$E_p < E_{q1}$	$E_p < E_{q2}$
0	$b_{00}$	7.64E+01	3.36E-00
0	$b_{01}$	-4.21E+01	-3.80E-00
0	$b_{02}$	7.67E-00	1.84E-00
1	$b_{10}$	4.63E+01	2.19E-00
1	$b_{11}$	-9.75E-00	-1.56E-00
2	$b_{20}$	2.66E+01	-1.94E+01
3	$b_{30}$	1.04E+02	-2.49E+02
4	$b_{40}$	-6.50E+02	-9.05E+02

Proton energy given in MeV (LAB)

TABLE IV. THEORETICAL DESCRIPTION OF THE pT DIFFERENTIAL ELASTIC SCATTERING CROSS-SECTION  $\sigma$  ( $\theta, E_p$ ) RELATIVE TO THE ANGLE  $\theta$  (CM) AND THE ENERGY  $E_p$  (LAB)

No.	$\theta$ , degrees	$E_p$ , MeV	$\sigma_{\text{theor}}$	$\sigma_{\text{exp}}$	$(\sigma_{\text{exp}} - \sigma_{\text{theor}})/\sigma_{\text{exp}}, \%$	Err (exp.)
1	5.86E+01	2.12	1.66E-01	1.80E-01	7.77E+00	9.00E-02
2	6.48E+01	2.12	1.49E-01	1.70E-01	1.25E+01	8.50E-02
3	9.00E+01	2.12	1.13E-01	1.08E-01	-4.26E+00	5.40E-02
4	1.10E+02	2.12	1.33E-01	1.27E-01	-4.72E+00	6.40E-02
5	1.25E+02	2.12	1.71E-01	1.76E-01	2.90E+00	7.80E-02
6	1.36E+02	2.12	2.04E-01	2.13E-01	4.42E+00	1.07E-01
7	5.47E+01	2.54	2.16E-01	2.32E-01	6.83E+00	1.15E-01
8	5.86E+01	2.54	1.98E-01	2.05E-01	3.36E+00	1.03E-01
9	6.48E+01	2.54	1.71E-01	1.87E-01	8.81E+00	9.50E-02
10	9.00E+01	2.54	1.04E-01	1.08E-01	3.09E+00	5.30E-02
11	9.63E+01	2.54	1.02E-01	1.01E-01	-5.83E-01	5.10E-02
12	1.10E+02	2.54	1.12E-01	1.03E-01	-8.80E+00	5.10E-02
13	1.25E+02	2.54	1.45E-01	1.39E-01	-4.32E+00	6.80E-02
14	1.36E+02	2.54	1.77E-01	1.76E-01	-3.83E-01	8.80E-02
15	1.52E+02	2.54	2.23E-01	2.39E-01	6.63E+00	1.20E-01
16	5.47E+01	2.74	2.31E-01	2.32E-01	4.23E-01	1.16E-01
17	5.86E+01	2.74	2.10E-01	2.08E-01	-9.66E-01	1.04E-01
18	6.48E+01	2.74	1.78E-01	1.95E-01	8.66E+00	9.80E-02
19	7.68E+01	2.74	1.29E-01	1.29E-01	2.86E-01	6.45E-02
20	8.00E+01	2.74	1.19E-01	1.15E-01	-3.46E+00	5.75E-02
21	9.00E+01	2.74	9.91E-02	1.03E-01	3.32E+00	5.13E-02
22	9.63E+01	2.74	9.43E-02	9.80E-02	3.81E+00	4.90E-02
23	1.10E+02	2.74	1.01E-01	9.40E-02	-7.29E+00	4.70E-02
24	1.25E+02	2.74	1.31E-01	1.34E-01	2.52E+00	6.70E-02
25	1.36E+02	2.74	1.61E-01	1.74E-01	7.38E+00	8.70E-02
26	1.52E+02	2.74	2.08E-01	2.18E-01	4.72E+00	1.09E-01
27	1.69E+02	2.74	2.42E-01	2.41E-01	-2.35E-01	1.20E-01
28	5.47E+01	3.03	2.42E-01	2.40E-01	-9.11E-01	1.20E-01
29	5.86E+01	3.03	2.18E-01	2.12E-01	-2.78E+00	1.06E-01
30	6.48E+01	3.03	1.81E-01	1.90E-01	4.53E+00	9.50E-02
31	7.68E+01	3.03	1.25E-01	1.41E-01	1.13E+01	7.05E-02
32	8.00E+01	3.03	1.14E-01	1.24E-01	8.18E+00	6.30E-02
33	9.00E+01	3.03	9.00E-02	9.50E-02	5.32E+00	4.76E-02
34	9.63E+01	3.03	8.29E-02	9.20E-02	9.88E+00	4.60E-02
35	1.10E+02	3.03	8.54E-02	8.50E-02	-5.14E-01	4.25E-02
36	1.25E+02	3.03	1.12E-01	1.07E-01	-4.84E+00	5.30E-02

37	1.36E+02	3.03	1.41E-01	1.40E-01	-6.77E-01	7.00E-02
38	1.52E+02	3.03	1.87E-01	1.86E-01	-5.78E-01	8.80E-02
39	1.69E+02	3.03	2.23E-01	2.21E-01	-1.10E+00	1.15E-01
40	6.00E+01	3.11	2.09E-01	1.74E-01	-2.02E+01	1.39E-01
41	7.00E+01	3.11	1.53E-01	1.13E-01	-3.53E+01	9.04E-02
42	8.00E+01	3.11	1.12E-01	8.50E-02	-3.14E+01	6.80E-02
43	9.00E+01	3.11	8.72E-02	7.40E-02	-1.78E+01	5.92E-02
44	1.00E+02	3.11	7.82E-02	7.50E-02	-4.20E+00	6.00E-02
45	1.10E+02	3.11	8.22E-02	8.00E-02	-2.71E+00	6.40E-02
46	1.20E+02	3.11	9.68E-02	8.80E-02	-9.96E+00	7.04E-02
47	5.47E+01	3.25	2.41E-01	2.42E-01	2.31E-01	1.21E-01
48	5.86E+01	3.25	2.16E-01	2.19E-01	1.53E+00	1.95E-01
49	6.48E+01	3.25	1.77E-01	1.84E-01	3.63E+00	9.20E-02
50	7.68E+01	3.25	1.19E-01	1.30E-01	8.63E+00	6.50E-02
51	8.00E+01	3.25	1.07E-01	1.15E-01	6.74E+00	5.75E-02
52	9.00E+01	3.25	8.24E-02	9.30E-02	1.15E+01	4.65E-02
53	9.63E+01	3.25	7.47E-02	8.00E-02	6.60E+00	4.00E-02
54	1.10E+02	3.25	7.59E-02	7.60E-02	1.42E-01	3.80E-02
55	1.25E+02	3.25	1.01E-01	9.95E-02	-1.18E+00	4.99E-02
56	1.36E+02	3.25	1.30E-01	1.35E-01	4.05E+00	6.65E-02
57	1.52E+02	3.25	1.77E-01	1.90E-01	6.72E+00	9.50E-02
58	1.69E+02	3.25	2.14E-01	2.16E-01	8.11E-01	1.08E-01
59	5.47E+01	3.50	2.32E-01	2.43E-01	4.48E+00	1.22E-01
60	5.86E+01	3.50	2.06E-01	2.08E-01	1.13E+00	1.04E-01
61	6.48E+01	3.50	1.67E-01	1.84E-01	9.27E+00	8.70E-02
62	8.00E+01	3.50	9.80E-02	1.14E-01	1.40E+01	5.70E-02
63	9.00E+01	3.50	7.41E-02	8.60E-02	1.39E+01	4.30E-02
64	9.63E+01	3.50	6.68E-02	7.40E-02	9.74E+00	3.70E-02
65	1.10E+02	3.50	6.80E-02	6.50E-02	-4.60E+00	3.35E-02
66	1.25E+02	3.50	9.21E-02	9.10E-02	-1.22E+00	4.55E-02
67	1.36E+02	3.50	1.21E-01	1.20E-01	-6.35E-01	6.00E-02
68	1.52E+02	3.50	1.69E-01	1.60E-01	-5.84E+00	8.00E-02
69	1.69E+02	3.50	2.08E-01	2.03E-01	-2.48E+00	1.02E-01
70	6.00E+01	3.51	1.96E-01	1.66E-01	-1.80E+01	1.33E-01
71	7.00E+01	3.51	1.38E-01	1.06E-01	-3.06E+01	8.48E-02
72	8.00E+01	3.51	9.76E-02	8.00E-02	-2.20E+01	6.40E-02
73	9.00E+01	3.51	7.37E-02	6.70E-02	-1.01E+01	5.36E-02
74	1.00E+02	3.51	6.48E-02	6.70E-02	3.34E+00	5.36E-02
75	1.10E+02	3.51	6.82E-02	7.20E-02	5.32E+00	5.76E-02
76	1.20E+02	3.51	8.18E-02	8.00E-02	-2.24E+00	6.40E-02
77	6.00E+01	3.83	1.76E-01	1.60E-01	-9.82E+00	1.28E-01

78	7.00E+01	3.83	1.22E-01	1.02E-01	-1.92E+01	8.16E-02
79	8.00E+01	3.83	8.51E-02	7.60E-02	-1.20E+01	6.08E-02
80	9.00E+01	3.83	6.48E-02	6.20E-02	-4.44E+00	4.96E-02
81	1.00E+02	3.83	5.78E-02	6.10E-02	5.23E+00	4.88E-02
82	1.10E+02	3.83	6.18E-02	6.50E-02	4.93E+00	5.20E-02
83	1.20E+02	3.83	7.50E-02	7.40E-02	-1.31E+00	5.92E-02
84	6.00E+01	4.19	1.51E-01	1.55E-01	2.36E+00	1.24E-01
85	7.00E+01	4.19	1.03E-01	9.80E-02	-5.08E+00	7.84E-02
86	8.00E+01	4.19	7.31E-02	7.20E-02	-1.52E+00	5.76E-02
87	9.00E+01	4.19	5.75E-02	5.60E-02	-2.60E+00	4.48E-02
88	1.00E+02	4.19	5.24E-02	5.40E-02	2.90E+00	4.32E-02
89	1.10E+02	4.19	5.59E-02	5.70E-02	2.00E+00	4.56E-02
90	1.20E+02	4.19	6.67E-02	6.80E-02	1.97E+00	5.44E-02
91	6.00E+01	4.60	1.31E-01	1.48E-01	1.13E+01	1.18E-01
92	7.00E+01	4.60	9.00E-02	9.50E-02	5.27E+00	7.60E-02
93	8.00E+01	4.60	6.76E-02	6.60E-02	-2.46E+00	5.28E-02
94	9.00E+01	4.60	5.54E-02	5.00E-02	-1.08E+01	4.00E-02
95	1.00E+02	4.60	4.90E-02	4.60E-02	-6.57E+00	3.68E-02
96	1.10E+02	4.60	4.75E-02	5.00E-02	5.00E+00	4.00E-02
97	1.20E+02	4.60	5.11E-02	5.00E-02	-2.15E+00	4.00E-02

Note:  $\sigma_{\text{theor}}$  is the theoretical cross-section value,  $\sigma_{\text{exp}}$  is the experimental cross-section value; the cross-sections are given in barns per steradian.

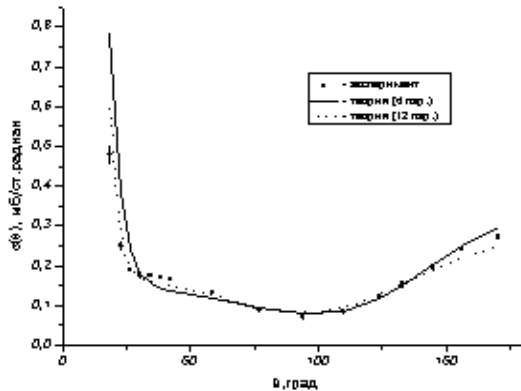


FIG. 1. Description of  $p+^3\text{He}$  elastic scattering according to Ref. [13] at  $E_p=4$  MeV. Legend: x-axis -  $\theta$ , degrees; y-axis -  $\sigma(\theta)$ , mb/steradian; ■ - experiment; - - theory (4 parameters); ... - theory (12 parameters).

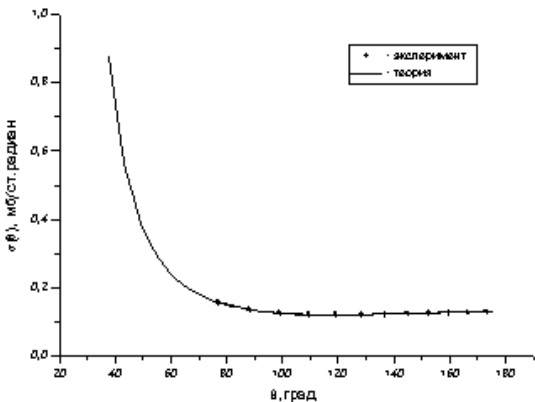


FIG. 3. Description of  $p+^3\text{He}$  elastic scattering at  $E_p=1$  MeV according to the authors' theory. Legend: x-axis -  $\theta$ , degrees; y-axis -  $\sigma(\theta)$ , mb/steradian; + - experiment; - - theory.

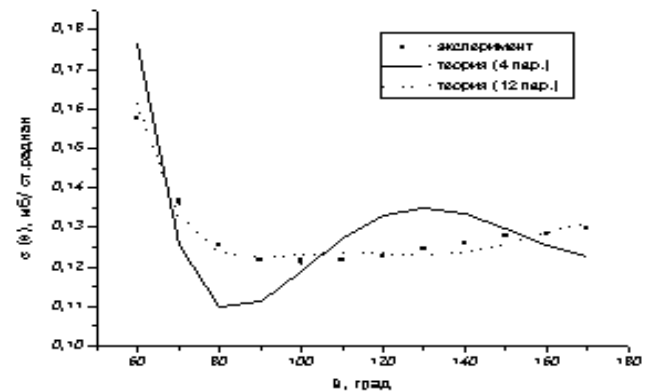


FIG. 2. Description of  $p+^3\text{He}$  elastic scattering according to Ref. [13] at  $E_p=1$  MeV. Legend: x-axis -  $\theta$ , degrees; y-axis -  $\sigma(\theta)$ , mb/steradian; ■ - experiment; - - theory (4 parameters); ... - theory (12 parameters).

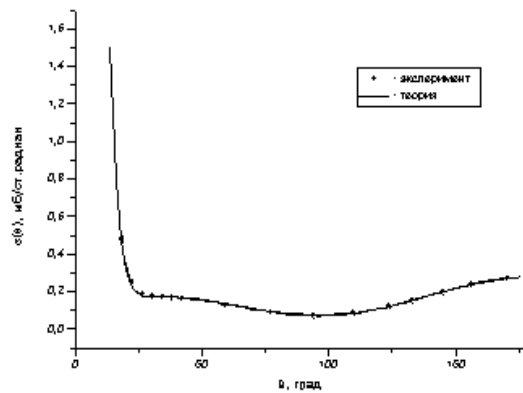


FIG. 4. Description of  $p+^3\text{He}$  elastic scattering at  $E_p=4$  MeV according to the authors' theory. Key: x-axis -  $\theta$ , degrees; y-axis -  $\sigma(\theta)$ , mb/steradian; + - experiment; - - theory.

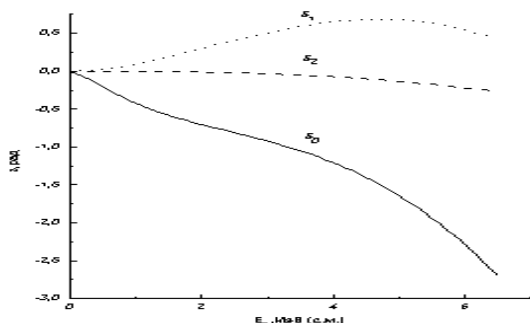


FIG. 5. The  $p+^3\text{He}$  elastic scattering phase shifts relative to energy. Legend: x-axis -  $E_p$ , MeV (CM); y-axis -  $\delta$ , rad.

## REFERENCES

- [1] DAVYDOV, A.S., Theory of the Atomic Nucleus, FML, Moscow (1958) Chapter 8.
- [2] ABRAMOVICH, S.N., GUZHOVSKIY, B.Ya., LAZAREV, L.M., Fizika Ehlementarnykh Chastits i Atomnogo Jadra **23** 2 (1992) 305.
- [3] GUZHOVSKIY, B.Ya., LAZAREV, L.M., ERSHOV, A.V., Izvestiya Akademii Nauk SSSR, Seriya Fizicheskaya **52** (1988) 61.
- [4] GUZHOVSKIY, B.Ya., ERSHOV, A.V., LAZAREV, L.M., Izvestiya Akademii Nauk SSSR, Seriya Fizicheskaya **54** (1990) 155.
- [5] MALMBERG, P.R., Phys. Rev. **101** (1956) 114.
- [6] LAZAREV, L.M., Ukrayins'kij Fizichnyj Zhurnal **36** (1991) 661.
- [7] AJZENBERG-SELOVE, F., Nucl. Phys. **A490** (1988), 1.
- [8] FESHBACH, H., Ann. Phys. **5** (1958) 357.
- [9] ABULAFFIO, C., PERES, A., in Proc. of Conf. Nucl. Cross Section and Technol., Washington (1975) 701.
- [10] WIGNER, P.R., Phys. Rev. **73** (1948) 1002.
- [11] BARIT, I.Ya., SERGEEV, V.A., Jadernaya Fizika **13** (1971) 1230.
- [12] FRANK, R.M., GAMMEL, J.L., Phys. Rev. **99** (1955) 1406.
- [13] TOMBRELLO, T.A., MILLER JONES, C., PHILLIPS, G.C., et al., Nucl. Phys. **39** (1962) 541.
- [14] ALLEY, M.T., KNUTSON, L.D., Phys. Rev. **C48** (1993) 1901.
- [15] BALDIN, A.M., GOL'DANSKIJ, V.I., ROZENTAL', I.L., Kinematics of Nuclear Reactions, Fizmatgiz, Moscow (1959) 147.
- [16] LANDAU, L.D., LIFSHITS, E.M., Quantum Mechanics, Gos. Izd. FML, Moscow (1963).
- [17] BAZ', A.I., ZEL'DOVICH, Ya.B., PERELOMOV, A.M., Reaction Scattering and Decay in Non-Relativistic Quantum Mechanics, "Nauka", FML, Moscow (1971) Chapter IX.
- [18] MERKUR'EV, S.P., Jadernaya Fizika **24** (1976) 289.
- [19] TILLEY, D.R., WELLER, H.R., HALE, G.M., Nucl. Phys., **A541** (1992) 1.
- [20] BERG, H., ARHOLD, W., HUTTEL, E., et al., Nucl. Phys. **A334** (1980) 21.
- [21] DRIGO, L., MANDUCHI, C., NARDELLI, G.C., et al., Nucl. Phys. **89** (1966) 632.
- [22] Mc DONALD, D.G., HAEBERLI, W., MORROW, L.W., Phys. Rev. **133** (1964) 1178.
- [23] CLASSEN, R.S., BROWN, R.J.S., FREIER, G.D., et al., Phys. Rev. **82** (1951) 589.
- [24] MANDUCHI, C., MOSCHINI, G., TORNELLI, G., ZANNONI, G., Nuovo Cimento, **LVIIB**, No 2, 340.
- [25] IVANOVICH, M., YOUNG, P.G., OHLSEN, G.G., Nucl. Phys. **A110** (1968) 441.

---

Nuclear Data Section  
International Atomic Energy Agency  
P.O. Box 100  
A-1400 Vienna  
Austria

e-mail: services@iaeand.iaea.or.at  
fax: (43-1) 26007  
cable: INATOM VIENNA  
telex: 1-12645  
telephone: (43-1) 2600-21710

---

Online: TELNET or FTP: iaeand.iaea.or.at  
username: IAEANDS for interactive Nuclear Data Information System  
usernames: ANONYMOUS for FTP file transfer;  
FENDL2 for FTP file transfer of FENDL-2.0;  
RIPL for FTP file transfer of RIPL;  
NDSOOL for FTP access to files sent to NDIS "open" area.

---

Web: <http://www-nds.iaea.or.at>